

## REVIEW SUMMARY

## METROLOGY

## Optical frequency combs: Coherently uniting the electromagnetic spectrum

Scott A. Diddams\*, Kerry Vahala\*, Thomas Udem\*

**BACKGROUND:** The generation and control of coherent electromagnetic waves, such as those provided by electronic oscillators in the radio frequency domain or lasers in the optical domain, have had an unparalleled impact on human society over the past century. For example, precise timing with radio waves referenced to atomic transitions undergirds navigation with the Global Positioning System. And modern communication systems are built around the properties of such waves to carry data through the air or within optical fibers that circumnavigate the globe. Such technical advances rely upon an exceptionally well developed and unified theoretical understanding of radio and optical waves, as well as the devices for their generation and control. Nonetheless and surprisingly, just 20 years ago, radio and optical technology realms remained largely distinct and isolated from one another. Although light waves could be modulated at radio rates and likewise electrical currents could be produced by demodulating optical signals, a simple coherent connection between radio and optical fields did not exist. As a result, many common technologies for the synthesis and control of radio frequencies, including those central to navigation, communications, and

measurement, seemed futuristic for optics. Conversely, the full potential of optics for time standards, metrology, and science was not accessible, despite a decades-long recognition of the opportunities and attempts to harness their technological impact. This situation, which arose as a consequence of the enormously high frequencies of electromagnetic waves in the optical domain, thereby limited scientific progress and technical capabilities.

**ADVANCES:** The invention of the laser in 1960 represented an optical analog to radio oscillators, which were invented much earlier. This development motivated efforts to create a coherent bridge between the radio and optical realms with multiple oscillators of successively higher frequencies being chained together. However, the sheer complexity and size of such approaches made it clear that these systems would never be widely available and that their capability would be limited. Such efforts were upended after nearly four decades of work when an unanticipated breakthrough enabled by combined advances in femtosecond laser technology, nonlinear optics, and precision frequency metrology finally solved this problem. The key to overcoming these issues was a new approach to

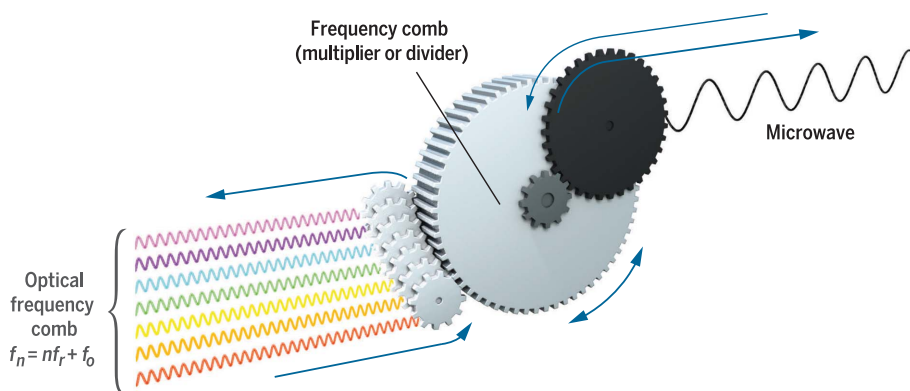
generate and control the spectrum of a mode-locked laser, which was called an optical frequency comb in accordance with the regularly spaced comb of frequencies it contained. Even though mode-locked lasers and optical frequency combs had existed previously, in 2000

## ON OUR WEBSITE

Read the full article at <https://dx.doi.org/10.1126/science.aay3676>

it was demonstrated how their spectra could be expanded over an octave of optical bandwidth. This critical advance enabled the technique of self-referencing, by which the optical frequencies of the comb are locked in an absolute sense to a radio frequency reference. In a simple and elegant way, this produced an optical clockwork, analogous to a gearbox (see the figure), that provided the bidirectional coherent connection between the optical and radio frequency domains. Moreover, because this connection is simultaneously established to many thousands of optical frequencies within the comb, self-referencing makes the coherent translation of frequencies possible across hundreds of terahertz of the optical spectrum.

**OUTLOOK:** In the two decades since the introduction of the frequency comb, entirely new scientific and technology vistas have been opened. New applications are leveraging an unprecedented sharing of the respective strengths of electronics and photonics, as well as a new freedom to work seamlessly across the broad optical frequency expanse. Frequency combs are used to realize and compare ultra-precise optical clocks at the 19th decimal place, which provides powerful approaches to test relativity and quantum theory as well as the search for physics beyond our present understanding. In addition, combs transfer this exceptional precision across the spectrum to perform massively parallel spectroscopy, generate the lowest-noise microwaves and few-cycle attosecond waveforms, and even help astronomers search for Earth-like exoplanets. Just as applications of frequency combs have expanded, there are new developments in frequency comb technology. Among these are combs that do not use mode locking for comb formation, as well as new approaches built on integrated photonics and microresonators that enable frequency combs on a silicon chip. Indeed, it is now clear that the once-enormous gap between optics and electronics will be further blurred as the coherent electromagnetic spectrum is united by frequency combs. ■



**An optical clockwork.** A frequency comb is a type of laser that functions in a manner analogous to a set of gears, as illustrated here, to link radio frequencies to a vast array of optical frequencies ("the comb") with values precisely determined by the expression  $f_n = nf_r + f_0$ , where  $f_r$  and  $f_0$  are radio frequencies and  $n$  is an integer on the order of  $10^5$ .

The list of author affiliations is available in the full article online. \*Corresponding author. Email: [scott.diddams@nist.gov](mailto:scott.diddams@nist.gov) (S.A.D.); [vahala@caltech.edu](mailto:vahala@caltech.edu) (K.V.); [thu@mpq.mpg.de](mailto:thu@mpq.mpg.de) (T.U.) Cite this article as S. A. Diddams *et al.*, *Science* **369**, eaay3676 (2020). DOI: 10.1126/science.aay3676

## REVIEW

## METROLOGY

# Optical frequency combs: Coherently uniting the electromagnetic spectrum

Scott A. Diddams<sup>1,2\*</sup>, Kerry Vahala<sup>3\*</sup>, Thomas Udem<sup>4\*</sup>

Optical frequency combs were introduced around 20 years ago as a laser technology that could synthesize and count the ultrafast rate of the oscillating cycles of light. Functioning in a manner analogous to a clockwork of gears, the frequency comb phase-coherently upconverts a radio frequency signal by a factor of  $\approx 10^5$  to provide a vast array of evenly spaced optical frequencies, which is the comb for which the device is named. It also divides an optical frequency down to a radio frequency, or translates its phase to any other optical frequency across hundreds of terahertz of bandwidth. We review the historical backdrop against which this powerful tool for coherently uniting the electromagnetic spectrum developed. Advances in frequency comb functionality, physical implementation, and application are also described.

Electromagnetic waves, whether microwave signals transmitted by a cellular phone or visible light given off by a lamp, are governed by Maxwell's equations. However, this unified physical framework belies a technological disparity between the electronic and the optical bands of the electromagnetic (EM) spectrum: Optical frequencies are far too fast to count, measure, and phase-coherently control in a manner that has become routine for the EM signals at electronic rates (hereafter also called radio or microwave frequencies). This difference in frequency of a factor of  $10^5$  is more than an obvious fact; it has led to a scientific and technological gulf between the radio and optical realms over the history of human-generated and -controlled EM oscillators that began with the revolutionary experiments of Hertz (1) (Fig. 1).

This gap has limited scientific and technical capabilities, as there was not a straightforward means to accurately connect the frequency and phase of optical oscillators to those in electronic circuits. Notably, in the field of time-keeping and frequency standards, this meant that there was no counting mechanism for clock oscillators at hundreds of terahertz that were long predicted to be more accurate and precise than their microwave counterparts. Moreover, even though frequency is the most precisely measured physical quantity, optical spectroscopy of energy eigenstates in atoms and molecules had to rely on much less accurate interferometric measurements of wave-

length. In some cases, this limited tests of fundamental physics. And although lasers existed since the 1960s and have proven to be exceptionally efficient carriers of data in long-haul fiber telecommunications networks, the agility with which optical waves can be synthesized, controlled, and manipulated falls short of the analog and digital radio frequency techniques that underlie modern cellular and computer networks.

This situation was radically changed around the turn of the century with the introduction of optical frequency combs that provided an elegant way to coherently unite the electromagnetic spectrum. Frequency combs provide a coherent and bidirectional link between radio frequency electronics and optics. The technologies belonging to these disparate realms underlie the key technical advancements of this age, and a sharing of their performance and other attributes has been enabled by the frequency comb linkage. Not surprisingly, the resulting unification of the EM spectrum has, in the brief 20 years since the introduction of the frequency comb, unleashed enormous new capabilities and created unforeseen technologies, the impact of which was both recognized and foreshadowed in awarding one-half of the 2005 Nobel Prize in Physics to Theodor Hänsch and John Hall (2, 3).

## Beginnings: Connecting the radio and optical domains

In 1886, Heinrich Hertz succeeded in artificially generating short bursts of radio waves and detecting them at a few meters' distance by observing sparks in an antenna-like structure (1, 4). This discovery was inspired by Maxwell's equations (5) that had predicted the existence of electromagnetic waves 13 years earlier. It took several decades until oscillators based on vacuum-tube feedback were

introduced for generating continuous and controllable coherent waves (6). The possibility of generating and receiving radio waves changed the world and is still evolving, as evidenced by the continued advances in wireless communications.

Until 1960, only incoherent sources were available at the much higher frequencies of light. The first important step in gaining coherent control over optical frequencies was a landmark paper by Charles Townes and Arthur Schawlow in which they pointed out how to extend the radio frequency technology of the maser, which Townes and co-workers had introduced earlier (7), into the optical realm (8). The first realization of this "optical maser," the device that is now called a "laser," was made by Theodore Maiman (9). And like Hertz's radio source, it emitted pulses of radiation. Shortly thereafter, Ali Javan and co-workers built the first continuously operating laser (10) and could demonstrate that it generated coherent light waves by observing a beat note between two waves (11). Unfortunately, the beat notes allowed only measurement of the frequency difference between two lasers. What was then called the "absolute" optical frequency remained orders of magnitude too large to measure directly, as was possible for radio frequencies. As a result, the radio and optical frequency realms remained separated, as sketched in the left part of Fig. 1.

At the same time, it was realized that control of the laser light waves would open up many possibilities in science and technology. An important example would be the optical version of radio frequency atomic clocks that were in those early days built in the form of a maser. Using the much higher frequencies of optical transitions in atoms held promise for a substantial boost in clock accuracy because the faster rate slices time into finer intervals. However, available electronic counting devices were orders of magnitude too slow, and they remain so even today. Therefore, the idea emerged to connect the optical and radio frequency realms by inching through the vast gap separating them by successive multiplication of a radio frequency reference, such as one derived from a radio frequency atomic clock. Early efforts to measure the frequency of laser light reached the CN laser at 964, 312.3 MHz in 1967 (12). Through this and other work, the harmonic frequency chain was born (13, 14) as a complex radio-optical system that foreshadowed the introduction of the vastly simpler optical frequency comb nearly four decades later. Figure 2A explains the concept of the harmonic frequency chain, and Fig. 2B shows its most refined implementation that phase-coherently connected a radio frequency input with a visible laser output (15). Other approaches have been proposed to count optical

<sup>1</sup>Time and Frequency Division, National Institute of Standards and Technology, Boulder, CO, USA. <sup>2</sup>Department of Physics, University of Colorado, Boulder, CO, USA.

<sup>3</sup>T. J. Watson Laboratory of Applied Physics, California Institute of Technology, Pasadena, CA, USA. <sup>4</sup>Max-Planck-Institut für Quantenoptik, Garching, Germany.

\*Corresponding author. Email: scott.diddams@nist.gov (S.A.D.); vahala@caltech.edu (K.V.); thu@mpq.mpg.de (T.U.)

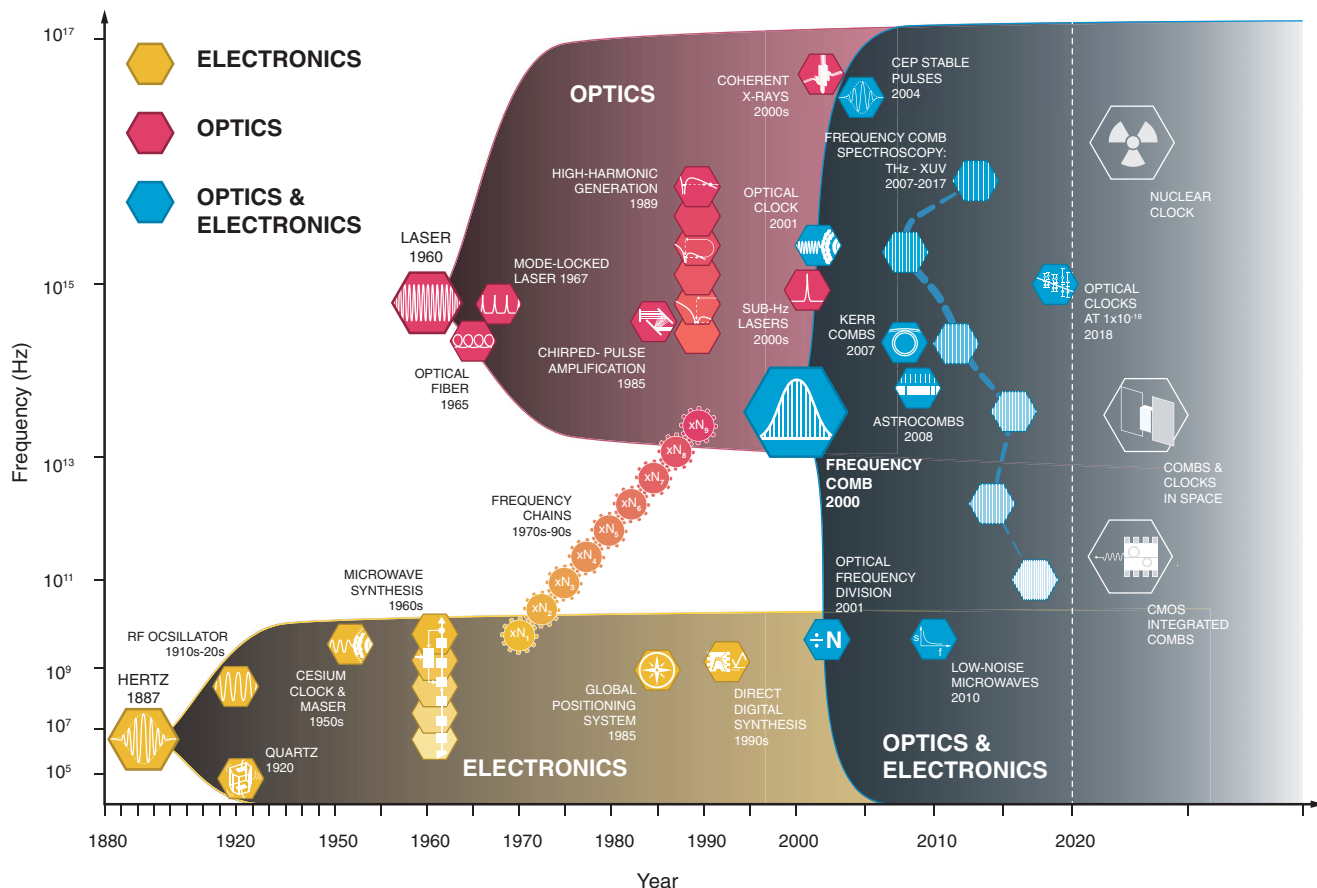


**Fig. 1. The coherent electromagnetic spectrum and its development.** In about 1887, Heinrich Hertz generated and detected artificial radio waves, which triggered a technological revolution that eventually gave birth to a plethora of systems for communications, navigation, and ranging (radar). Radio frequency (RF) masers and atomic clocks introduced in the 1950s were a technological game changer. The cesium atomic clock defines not only the second, but undergirds the International System of Units (SI) (20). With the introduction of the laser in 1960, the first source of coherent optical electromagnetic waves became available.

frequencies (16, 17) but thus far have not been realized.

Among the early applications of these efforts was an experiment to refine the value for the speed of light (18). This was possible using  $c = f\lambda$  where  $f$ , the optical frequency, was measured by using a harmonic frequency chain and  $\lambda$ , the wavelength, was determined by precision interferometry through comparison with the wavelength of a specific krypton transition (1960 definition of the meter). Ultimately, however, an improved realization of length was possible by defining the value of the speed of light to be exactly 299,792,458 m/s in the 1983 revision of the International System of Units (SI) (19, 20). Because frequency is, and always has been, the most accurately measured quantity in all of physics, this definition implies that, in theory, frequency-like accuracy could be obtained for length. In practice, a laser stabilized to a frequency-calibrated optical tran-

sition (21, 22) serves conclusively as a realization of the meter. Harmonic frequency chains were also used to determine transition frequencies in atomic hydrogen. These measurements tested quantum electrodynamics and determined the values of physical constants (23, 24). Not much more could be done with the harmonic frequency chains because they were large and very complicated systems containing many microwave and laser subsystems that needed to operate in a highly coordinated fashion. Their sheer complexity made it clear that these systems would never be widely available and that their capability would be limited.

Nonetheless, harmonic frequency chains inspired new approaches aimed at simplification. A key initial step in this direction was the optical interval divider, as proposed by Hänsch in 1989 (25) (Fig. 2, C to E). This device works in a way analogous to a differential gear except for optical frequencies, precisely bisect-

This big leap in technology, as well as in frequency, introduced a gap of about  $10^5$  relative to the highly controllable radio frequency domain. Harmonic frequency chains bridged this gap, but the resulting systems were impractical. The frequency comb, which was introduced in its fully functioning form in 2000, coherently united the radio and optical realms in a simple and practical way. It has opened many new possibilities such as optical atomic clocks, ultralow-noise microwaves, carrier-envelope phase control of ultrashort pulses, and the coherent synthesis of radiation ranging from terahertz to extreme ultraviolet.

ing an arbitrarily large frequency interval (see Fig. 2D). The optical interval divider could be concatenated to successively bisect the interval between an optical frequency  $f$  and its own second harmonic  $2f$  that can easily be obtained with nonlinear crystals. As described below, this idea was used later in a slightly different fashion in the operation of the modern optical frequency comb. An interval divider chain would have used roughly the same number of stabilized oscillators as a frequency chain. However, it offered an important advantage in that all the oscillators could have been of the same type, yielding an enormous reduction in complexity. At least two groups, at the Max Planck Institute of Quantum Optics, Germany (26), and the National Institute of Advanced Industrial Science and Technology, Japan (27), had started to construct such an interval divider chain, but these efforts were never completed.

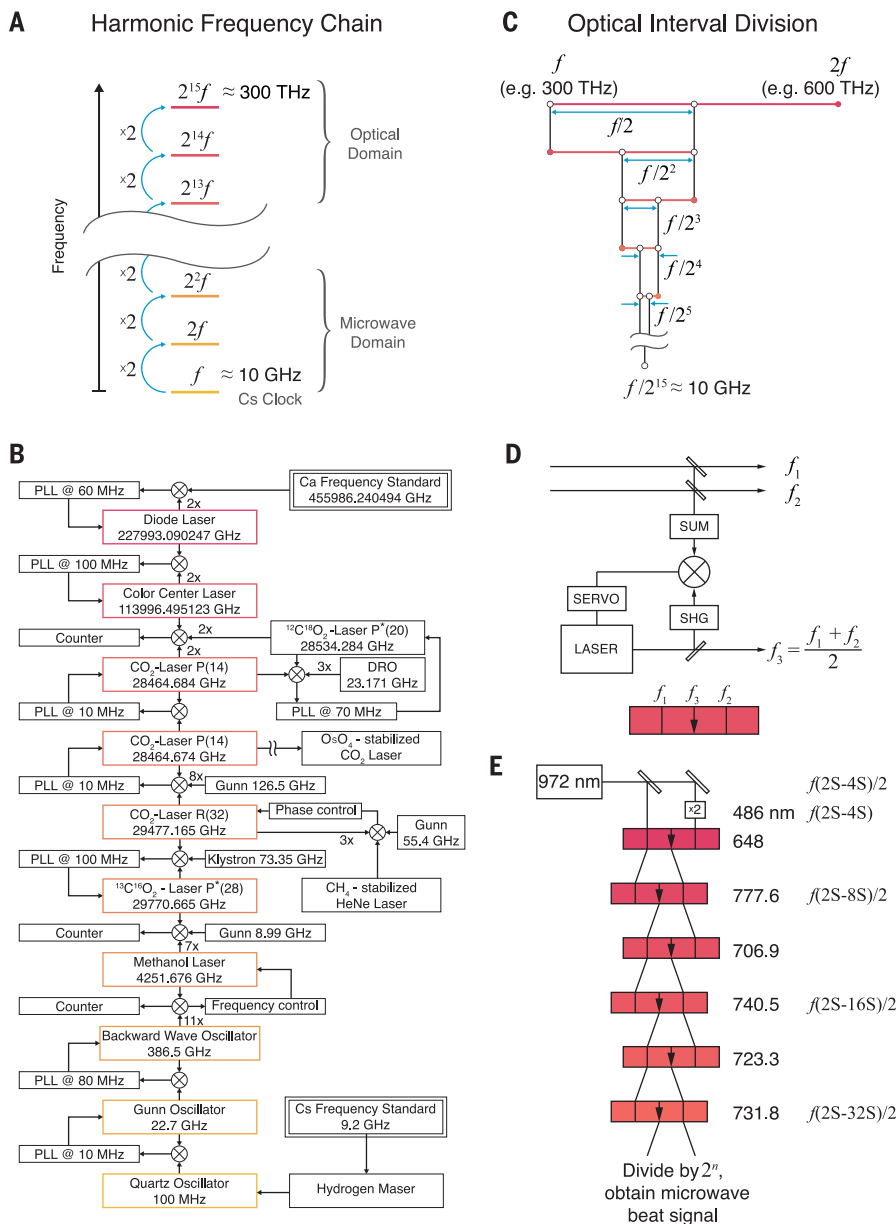


**Fig. 2. Historical approaches to connect optical and microwave domains.** (A) Successive nonlinear frequency multiplication with a harmonic frequency chain connecting radio and optical frequencies. For illustration, a factor of 2 in frequency separates each step. (B) Harmonic frequency chain implementation that existed at the Physikalisch Technische Bundesanstalt (PTB) at Braunschweig, Germany, and filled two large laboratories located in two different buildings [adapted from (15)]. Nonlinear devices generate harmonics in each step to which an intermediate oscillator is phase locked (PLL, phase-locked loop) to provide enough power for the next multiplication step. In this way one walks through the spectrum, from the microwave frequency of a cesium atomic clock all the way to the visible frequency of a calcium standard at 456 THz. The multiplicative factor between lower-frequency stages could be substantially larger than 2x. (C) As an alternative, one could converge to a radio frequency by successively bisecting the interval spanned by an optical frequency  $f$  and its own second harmonic  $2f$ . (D) An optical interval divider phase locks the second harmonic (SHG) of a laser at  $f_3$  to the sum frequency (SUM) of two input lasers at  $f_1$  and  $f_2$ , bisecting the frequency difference between the latter:  $f_3 = (f_1 + f_2)/2$ . (E) A proposed (25) but never realized implementation of an interval divider chain that would have been designed for application to atomic hydrogen. In agreement with the Rydberg formula, the transition frequencies are at small integer ratios, several of which (at the right hand side) agree with the frequencies in this interval divider chain. [(D) and (E) are adapted from (25).]

**An optical clockwork**

Around the turn of the millennium, the rapid advance in mode-locked lasers as optical frequency comb generators eliminated the need for harmonic frequency chains and optical frequency interval dividers. In a spectacular simplification, the frequency comb collapsed a dozen stages into a single direct link between an input radio frequency signal and a vast array of optically synthesized frequencies that are spaced on a perfectly even frequency grid extending over an octave of spectrum. Moreover, the comb phase coherently converts a radio frequency into an optical frequency with frequency multiplication by  $\approx 10^5$ , or in reverse, it divides by the same factor. In fact, in such a radio-to-optical conversion, both division and multiplication happen simultaneously. With the long-standing goal of frequency conversion readily at hand, one can now select the domain, radio or optical, in which the best oscillators exist and convert it to the other domain. And whereas the harmonic chains easily filled a few large laboratories and operated only occasionally, current frequency combs now fit in a shoe box and run continuously, thus finally realizing a straightforward means to unite the electromagnetic spectrum.

In a simple picture, the frequency comb can be associated with the longitudinal modes of a laser cavity that are separated by a frequency  $f_r$ . Comb formation relies on a nonlinear optical process, called mode-locking, to enforce equal frequency spacing and establish phase synchronization between the modes such that a short optical pulse is formed (Fig. 3A). This pulse propagates at its group velocity back and forth between the end mirrors of the laser resonator with a round trip time of  $f_r^{-1}$ . At each round trip, a copy of the pulse is transmitted through one of these mirrors that is partially transparent. The well-known Fourier transformation between time and frequency domain implies that the spectrum of the periodic pulse train generated in this way is in fact a discrete comb of frequencies. Moreover, the spectral width of the comb would approach the optical carrier frequency as the pulse duration is reduced to a single optical cycle.

Further technical details about the operation and generation of the frequency comb are provided in subsequent sections, but the range of ways that a frequency comb coherently connects the EM spectrum, whether from microwave to optical, optical to microwave, or optical to optical, is captured intuitively through the optical clockwork analogy illustrated in Fig. 3B. At its center is the frequency comb represented as a large gray gear that is enmeshed with a microwave source symbolized by the black gear. The frequency comb connects the microwave gear in a phase-coherent way, i.e., without slippage, to the smaller fast-spinning gears, each of them associated with a single optical

Downloaded from <http://science.sciencemag.org/> on July 16, 2020



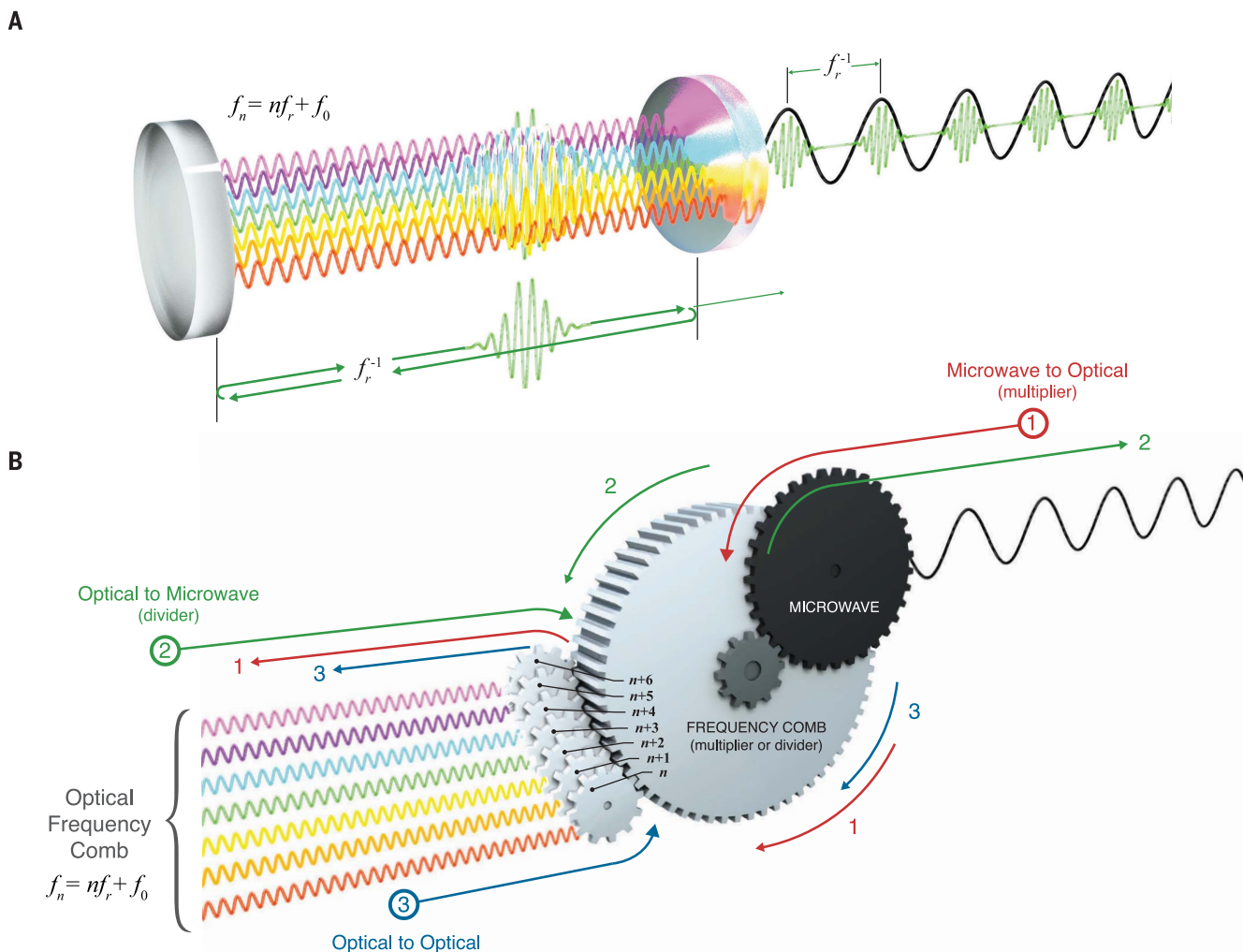


**Fig. 3. The frequency comb as an optical clockwork. (A)** An optical frequency comb, here illustrated as waves of different colors that are spatially separated for clarity, is composed of the longitudinal modes of an optical cavity made by two mirrors. The comb frequencies are given by  $f_n = nf_r + f_0$ . In reality the waves are spatially overlapped and phase synchronized such that their superposition produces a pulse circulating inside the cavity. The output of the cavity consists of a periodic train of replicas of the intracavity pulse separated by the round-trip time  $f_r^{-1}$ . **(B)** Mechanical analogy of the optical frequency comb. The frequency comb has three modalities in which it can operate to phase

coherently connect electronic (microwave) and the optical realms of the EM spectrum: 1. An input microwave frequency is multiplied by a factor of  $\sim 10^5$  to the optical domain, where it is output as an array of equally spaced light waves. 2. In the inverse of the first modality, an input high-frequency optical wave can be divided down to the microwave domain. 3. Spectral translation between the array of optical waves occurs when an input optical field controls the comb and is phase-coherently connected to the other frequencies in the optical domain. As shown, all modalities of operation are bidirectional and simultaneous.

frequency of the comb. Even though this clockwork shows only seven fast-spinning gears, an actual frequency comb would feature  $\approx 10^5$  of them covering a full octave. Also, the actual frequency ratios spanned by a comb are much larger than can be easily displayed in Fig. 3B. However, the clockwork illustrates the three major ways that the frequency comb enables coherence to be transferred or shared across the radio and optical spectra. Each of these operational modes has led to a broad application category of comb technology, as described below.

**Optical frequency synthesis**

The precise synthesis of new frequencies was required for the harmonic frequency

chain (Fig. 2B) and more broadly for the advancement of radio communications. In a radio frequency synthesizer, new frequencies are generated through various processes, including electronic multiplication and division, phase-locked loops, and direct digital synthesis. Optical frequency combs operating in mode 1 (red arrows in Fig. 3B) can be viewed as a pronounced extension of the concept of frequency synthesis from the radio to optical realms. Here, the frequency comb transfers the radio frequency coherence (black sinusoid) to a very broad spectrum of equally spaced optical frequencies  $f_n$  represented by the small gears. These frequencies are given by the expression (28–30)

$$f_n = nf_r + f_0 \tag{1}$$

As noted,  $f_r$  is the pulse repetition rate, or equivalently, the frequency separation of the comb modes, whereas  $f_0$  is an offset frequency that is common to all the modes and whose origin and measurement will be discussed in greater detail below. For many frequency combs, both  $f_r$  and  $f_0$  are typically in the range of 0.1 to 10 GHz, such that  $n = 10^4 \dots 10^6$  is the required multiplier for  $f_n$  being in the near-infrared frequency band. As a result, if  $f_r$  and  $f_0$  are stabilized to a known radio frequency reference, such as that provided by a cesium clock, then one obtains 100,000 stabilized lasers superimposed in one beam.

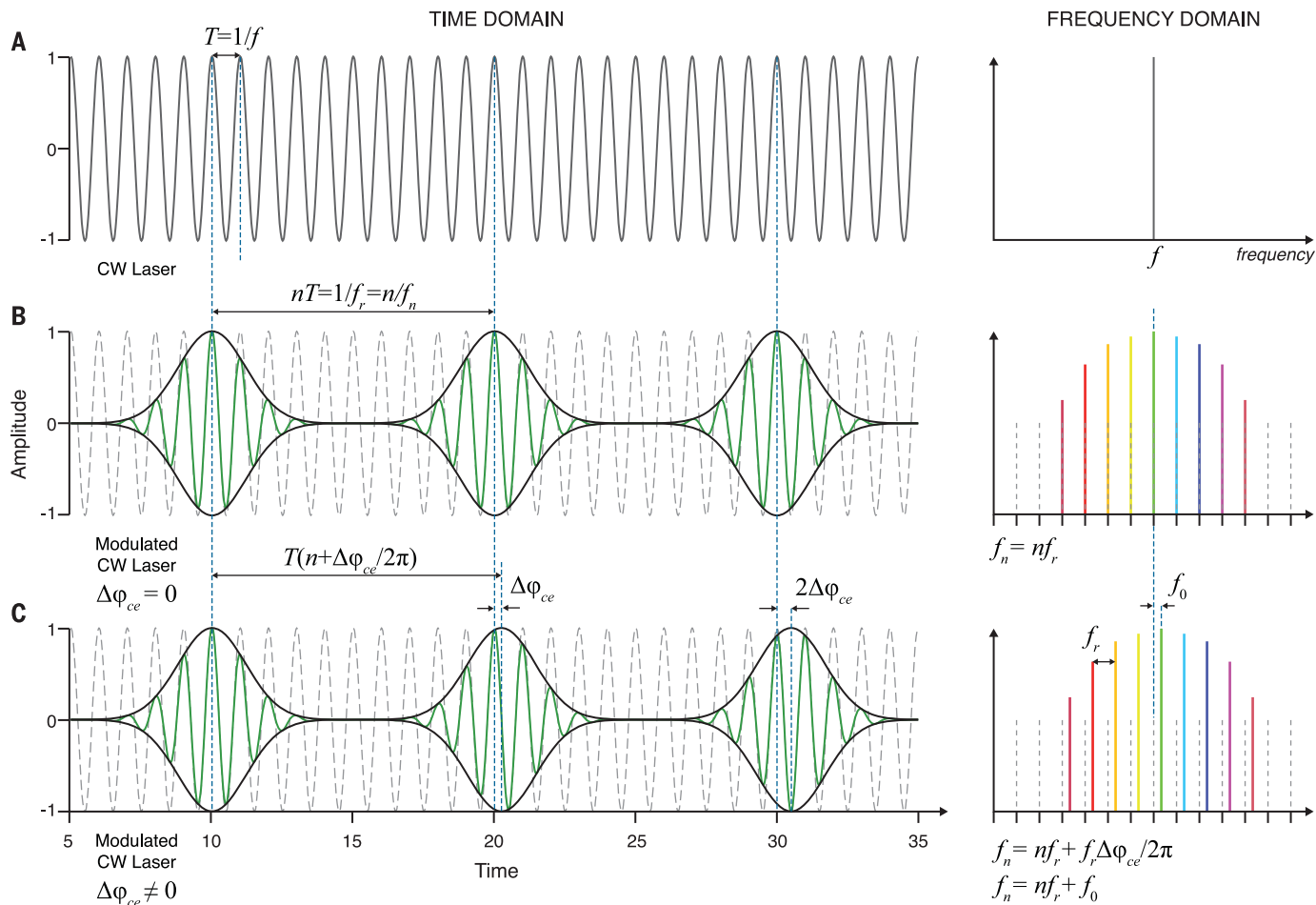


**Fig. 4. Time- and frequency-domain representations of the optical frequency comb.** (A) The continuous optical wave with frequency  $f$  and period  $T$  is represented as a single tone in the frequency domain. (B) An amplitude modulation on the optical wave at a lower frequency  $f_r$  that is an exact subharmonic of  $f$  would enable simple frequency division by an integer  $n$ . Here the modulation is shown at  $f/10$ . In reality, if  $f = 500$  THz, the modulation at  $f/10^5$  would yield a countable  $f_r = 5$  GHz. (C) In general, the modulation

frequency is not an exact subharmonic of  $f$ , but rather the modulation envelope “slips” with respect to the fixed carrier  $f$  from pulse to pulse. Here, for example, the slip is  $1/4$  of a cycle, so the modulation  $f_r = f/(10 + 1/4)$ . It is this noninteger portion of the denominator that causes the pulse-to-pulse carrier-envelope phase shift. In the frequency domain, the pulse-to-pulse phase shift results in a comb shifted by  $f_0 = f_r \Delta\phi_{ce}/(2\pi)$ . By measuring  $f_0$ , one can determine the noninteger part of the divisor exactly.

The first demonstrations of synthesis with laser frequency combs were published around the turn of the 21st century (31–34). These works showed the power of measuring and controlling  $f_r$  and  $f_0$ , as well as the ability to generate a comb of optical frequencies traceable to the microwave SI second. Moreover, they opened the gates to a flood of optical frequency measurements that served to validate the painstaking efforts from previous decades with the frequency chain technology; see, for example, (33, 35, 36). Although this was important for the metrology community and the development of optical frequency and length standards, new opportunities of a more fundamental nature also emerged. For example, a comparison of microwave (cesium) and optical frequency standards by means of the laser frequency comb can be interpreted as a test of the constancy of fundamental constants, such as the electron-to-proton mass

ratio and the fine-structure constant, either in space or time (37–39).

The ease with which any optical frequency could be measured has been extended to spectroscopy across the EM spectrum (40–42). Many such spectroscopy experiments use continuous-wave lasers that are simultaneously calibrated by a heterodyne measurement with the stabilized comb. But powerful approaches have also arisen in which the comb itself serves as an array of hundreds of thousands of individual lasers that simultaneously act as a spectroscopic probe (43–46). Coupling the frequency comb to another optical cavity is sometimes used to enhance the power of the relatively weak comb modes (often  $<100$  nW in a single comb mode), thus improving the spectroscopic sensitivity (47, 48). To read out the individual comb modes, clever detection schemes have been realized, including the use of a highly dispersive spectrometer (49) or a swept Vernier

cavity filter (50). Alternatively, the addition of a second frequency comb, offset slightly in repetition rate, forms a dual-comb spectrometer in which the amplitude and phase of individual optical modes are uniquely mapped to a radio frequency beat recorded on a single photodetector (51–57). Frequency comb spectroscopy (58, 59) is a rapidly growing subfield that is being applied to a wide range of basic and applied research topics. A noteworthy variation is the use of frequency combs to calibrate high-precision astronomical spectrographs aimed at identifying habitable exoplanets through the measurement of minute Doppler shifts in the stellar spectra (60–62).

#### Clocks and optical frequency division

A clock consists of an oscillator and a counting mechanism. This basic concept has been implemented throughout history with technology operating at ever-higher frequencies: beginning

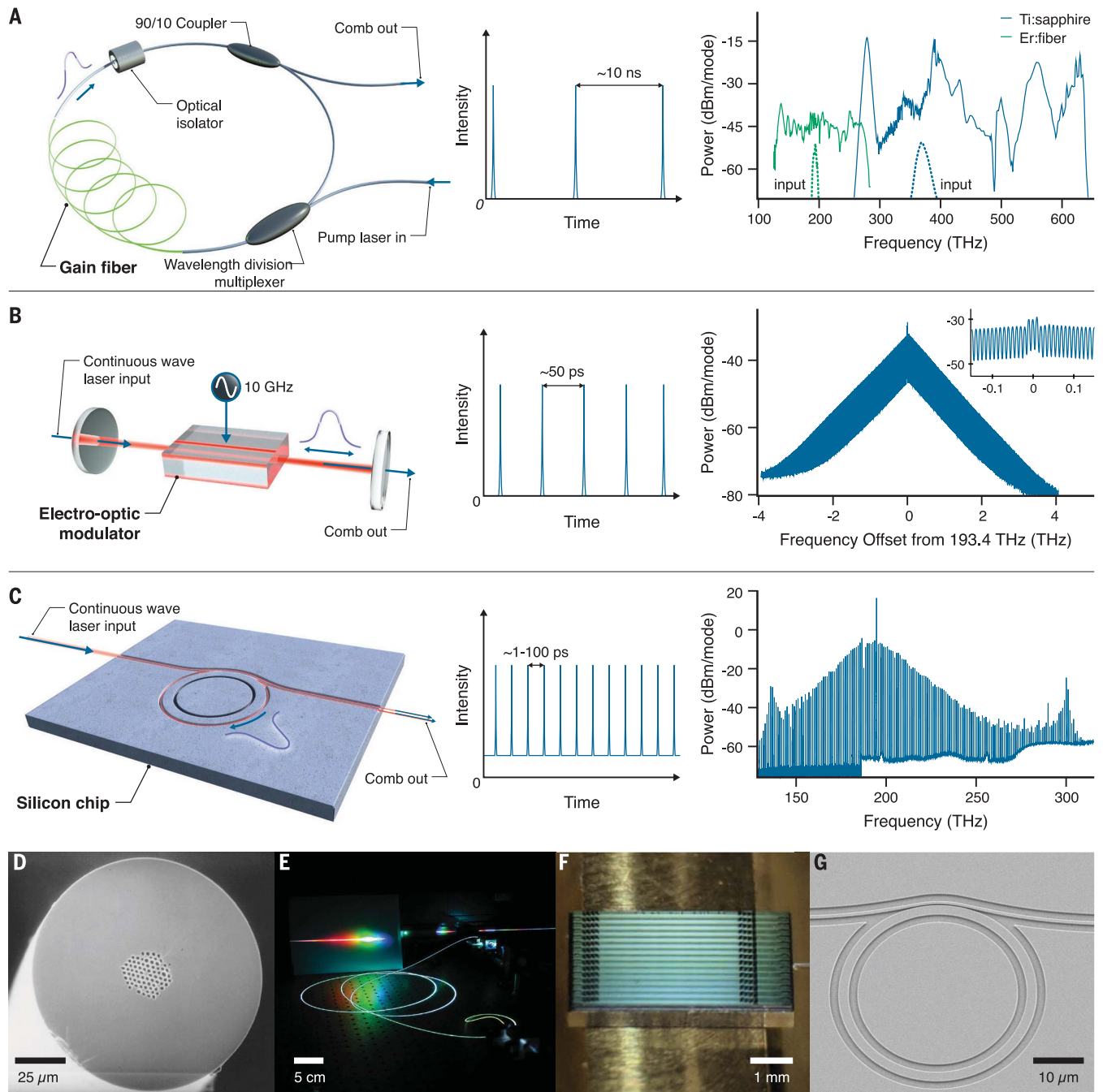


**Fig. 5. Methods for optical frequency comb generation.** (A) Mode-locked lasers. A pulse is stored within a cavity formed by an optical fiber loop. During each round trip, a fraction of the circulating pulse is coupled out, forming a pulse train with a typical period of 10 ns. Cavity losses are compensated by a gain medium, and an optical isolator ensures unidirectional operation. At right are typical spectra from such an Er:fiber laser, as well as a Ti:sapphire laser, both before and after spectral broadening to octave span in a nonlinear fiber. Comb modes are not resolved in these spectra. (B) Electro-optic comb generator. Microwave modulation creates an optical comb by adding sidebands to an injected carrier wave from a continuous-wave laser. The modulator is placed inside an optical cavity with free spectral range matched to the modulation frequency. The output pulse period is twice the modulation period, or 50 ps in

this typical example. The spectrum shown at right has a 10-GHz mode spacing. (C) Microresonator frequency comb. A frequency comb is generated by the nonlinear Kerr effect in a passive microfabricated waveguide cavity. The balance of dispersion and nonlinearity yields a stable soliton that circulates in the ring cavity with a typical period in the range of 1 to 100 ps. At right is the spectrum of the associated frequency comb with a spacing of 1 THz (172). (D to G) The images in the lower panels show key nonlinear optical technologies used to generate octave-spanning frequency combs. (D) Nonlinear microstructure fiber (97), and (E) the visible-light spectrum such fiber can produce (101). (F) A millimeter-sized silicon chip with 15 nonlinear silicon-nitride waveguides (173). (G) A silicon-nitride ring resonator on a silicon chip for generating the comb with 1-THz mode spacing (142, 172).



with the motion of Earth itself and progressing through pendulum clocks, quartz oscillators, and the microwave cesium clock. Along this historical path, a clear guiding principle in timekeeping has been to use the highest frequency possible for the clock oscillator, as this provides the opportunity to most precisely divide time into the smallest intervals. With amazing foresight, an optical time standard was already anticipated by Maxwell (5), even though he lived 100 years before the invention of the laser. And though a laser referenced to an atomic transition provides the pendulum of such an optical clock, until the frequency comb, there was no practical way to count the ultrafast cycles of optical light.

In the mechanical analogy of Fig. 3B, building an optical clock involves using the clockwork as indicated by the green arrows. In the actual laser frequency comb, the frequency of one of the comb modes  $f_n$  is controlled relative to the optical frequency reference,  $f_{\text{opt}}$  (e.g., a laser steered to an optical transition), such that Eq. 1 can be rewritten as

$$f_r = (f_{\text{opt}} - f_0)/n \quad (2)$$

Here, the readout of the optical clock is the repetition rate of the pulse train of the frequency comb laser, which is essentially a very large subharmonic of  $f_{\text{opt}}$  because  $f_0 \ll f_{\text{opt}}$ . Within a year of the introduction of the self-referenced frequency comb, such optical clocks had been implemented (63, 64), and their uncertainty was soon competitive with that of the best Cs microwave clocks. In addition to the frequency comb, there were two important scientific and technological advances at the end of the 1990s that accelerated the development of optical clocks and have elevated them to the peak of metrologic precision. The first was the maturation of laser cooling and trapping techniques proposed decades prior (65, 66) that now hold atoms essentially motionless to eliminate Doppler effects and allow the realization of atomic-transition quality factors exceeding  $10^{15}$ ; see, for example, (67). The second was the development of a new class of hertz-linewidth lasers based on vibration-insensitive mounting of the reference resonator (68, 69) that enabled operation at the fundamental thermodynamic limit (68, 70, 71).

The continued advancement of these technologies over the past 20 years has led to stabilized lasers with a linewidth of just a few tens of millihertz (7) and optical frequency standards and clocks with fractional frequency uncertainty pushing into the  $10^{-19}$  range (72–76). Beyond counting the cycles of such ultraprecise optical frequency references, optical frequency division of a cavity-stabilized laser with the comb now provides microwave signals with short-term stability and phase

noise that surpasses that of the lowest-noise microwave oscillators (77, 78). Indeed, optically generated microwaves with a frequency comb leverage the ultrahigh optical quality factors and narrow-linewidth lasers mentioned above, the equivalent of which are unavailable directly in the microwave realm. Finally, combinations of optical clocks and free-running ultrastable optical oscillators together with the frequency comb clockwork have recently been applied to the generation of optical time scales (79–82), which are beginning to play a role in coordinated universal time (UTC) and will someday realize a new definition of the SI second (83, 84).

#### Optical-to-optical coherence transfer

The superior performance of optical clocks and frequency standards has created a situation in which the SI definition of the second is now realized with a 100-times larger fractional uncertainty ( $1 \times 10^{-16}$ ) than the agreement found among the best optical clocks ( $1 \times 10^{-18}$ ) (73). This will ultimately be rectified with a future redefinition of the second in terms of an optical transition, but the present operational advantage for frequency synthesis is regularly realized by using an optical frequency to reference the comb. Not only does this provide optically stable microwaves, as just discussed, but it provides a means to synthesize other optical frequencies across hundreds of terahertz, or even petahertz, of bandwidth. This enormous range of synthesis bandwidth is displayed in Fig. 1, where it should be noted that the optical domain encompasses a bandwidth greater than the gap between radio frequency and optical realms. Previously, smaller gaps of a few terahertz in the optical realm could be bridged (85), but low-noise frequency comb sources have now connected the entire optical spectrum, with phase coherence being transferred between the multitude of comb modes (Fig. 3B, blue arrows).

One of the uses of optical coherence transfer is to compare the ratio of widely separated optical clock frequencies. Indeed, the most accurate and fastest means to evaluate uncertainty in the best optical clocks is to compare them, one against the other, by using the frequency comb. This process essentially amounts to measuring the ratio of optical frequencies (86). It was first demonstrated with the comparison of  $\text{Hg}^+$  and Ca optical clocks (63) but has since been extended to practically all high-performance clocks. As with the microwave-to-optical mode of operation, the ratio of optical frequencies can also be interpreted to constrain physical models in which the fine-structure constant  $\alpha$  is not in fact constant (87, 88). In addition, the same ratios of optical frequencies are being used in searches for dark matter and other new

physics (89, 90). From a more practical standpoint, the coherent control of the frequency comb spectrum has enabled optical time transfer between remote clocks with femto-second precision (91), and absolute ranging with nanometer-level precision over kilometer distances (92).

#### The carrier-envelope offset frequency

The mechanical analogy of the frequency comb presented in Fig. 3B is useful to understand its basic function and modes of operation, but it does not capture the physical origin and understanding of  $f_0$ , which is more generally called the carrier-envelope offset frequency. Indeed, if not for  $f_0$ , the synthesis from microwave to optical realms, and vice versa, would have been completed as depicted in Fig. 3 with the first mode-locked lasers in the 1960s. And though the origins of  $f_0$  were understood as early as the mid-1970s (28), it took until the 1990s to realize how to measure and control it in the context of an optical frequency comb.

To understand the implications of  $f_0$  for a frequency comb, it is helpful to first describe optical frequency division without it. Imagine the continuous light wave at a frequency  $f$  sketched in Fig. 4A to be amplitude modulated with a frequency  $f_r$ , as shown in Fig. 4B. In particular, the amplitude function is thought to produce a pulse of light exactly every  $n$  cycles of the continuous light wave. In this case, the lower (electronically countable) frequency  $f_r$  is an exact subharmonic such that  $f_r = f/n$ , and the associated optical frequency comb, would be  $f_n = nf_r$ . This time-frequency description of a modulated light wave was analogously depicted as the frequency-dividing clockwork in Fig. 3B.

However, the situation just described is not typically realized in frequency comb generators where dispersion in the optical cavity producing the comb gives rise to differing group and phase velocities. This causes the pulse envelope to be delayed relative to the carrier from pulse to pulse by the carrier-envelope phase slip  $\Delta\phi_{\text{ce}}$ . This phenomenon has an intuitive geometrical interpretation for well-behaved pulse shapes, as shown in Fig. 4C, and was experimentally verified in 1996 (93). The consequence of the pulse-to-pulse carrier-envelope phase slip in the frequency domain is to offset the entire frequency comb by an amount  $f_0 = f_r \Delta\phi_{\text{ce}} / (2\pi)$  (28). Here we recognize that  $\Delta\phi_{\text{ce}} / (2\pi)$  is the fraction of the optical cycle by which the envelope slips from pulse to pulse, making it possible to realize division of the optical frequency to the modulated envelope as  $f_r = f / (n + \Delta\phi_{\text{ce}} / (2\pi))$ , which is equivalent to Eq. 2.

Because  $f_r$  is the round-trip rate of pulses in the laser cavity, its measurement is straightforward by photo detection of the emitted laser pulses. A practical way to measure  $f_0$  is,



however, more challenging. Eventually this so called “self-referencing” is achieved with a nonlinear interferometer that heterodynes the second harmonic of a set of modes with indices near  $n_L$  from the low-frequency side of the comb spectrum with another set of modes near index  $n_H = 2n_L$  to generate the beat frequency  $2f_{n_L} - f_{n_H} = f_0$ . This “ $f - 2f$ ” method is seen to be a variation of the optical interval divider (Fig. 2, C to E) and could be implemented with a combination of a frequency comb and interval dividers (27). However, the most simple and efficient implementation (26, 94) requires an octave-spanning frequency comb that was not readily available in the 1990s. The solution to this issue was first presented by a new type of nonlinear optical fiber, commonly called microstructure or photonic crystal fiber (95, 96), that could be used to generate octave-spanning frequency combs using nanjoule-level pulses from the existing narrowband mode-locked lasers (97). This provided the key missing technology for the measurement of  $f_0$  and the closing of the clockwork that could then readily connect optical and microwave realms (32–34).

### Frequency comb technologies

The history of frequency comb technologies involves a rich combination of laser physics, ultrashort optical pulse generation, nonlinear optics, and electro-optics. In most cases, the core technologies that are now central to frequency combs were developed for independent and unrelated reasons, which highlights the importance of cross-disciplinary research in the growth of the frequency comb field. Some of the most common techniques for generating optical frequency combs and extending their spectral bandwidth are shown in Fig. 5.

#### Mode-locked laser frequency combs

The mode-locked laser was introduced just a few years after the 1960 invention of the laser itself (98). By the early 1980s, progress in the field had led to techniques for the generation of femtosecond time-scale pulses (99) that were primarily used for measuring ultrafast dynamics in material systems. A key element of a mode-locked laser is a means to favor the generation of short pulses of light inside the laser cavity. Initially, active amplitude modulation was used, but in most mode-locked lasers, pulses are now generated passively with a saturable absorber or another nonlinear element that provides a net increase in gain for pulsed operation. Once generated, pulses are stored on a repetitive path, either within a cavity formed by mirrors or an optical fiber loop, as shown in Fig. 5A. In steady state, the circulating pulse is approximated by a soliton that maintains its shape indefinitely through a balance of nonlinearity and dispersion. This produces a train of pulses with identical en-

velope at the laser output and results in the perfectly regular comb structure.

The first self-referenced frequency combs used Kerr-lens mode-locked Ti:sapphire lasers that had been introduced in 1990 (100) and matured over the subsequent decade. Example spectra are shown in Fig. 5A. Typical Ti:sapphire lasers have peak emission around 800 nm and emit pulses with duration <100 fs. This corresponds to a Fourier-limited spectral bandwidth >5 THz, which falls considerably short of the octave spectrum required for self-referencing and detection of  $f_0$ . Broadening to octave span uses the previously mentioned microstructure fiber. This fiber has air channels running along its length that increase optical confinement and hence optical nonlinearity. Moreover, the channels allow for new freedom in dispersion design to substantially enhance the spectral broadening of the low-energy (nanjoule) pulses (95, 96, 101) (Fig. 5D). Such fibers immediately enabled the generation of octave-spanning frequency combs from the existing Ti:sapphire lasers (see spectra of Fig. 5A), as required for self-referencing. With improved engineering, Ti:sapphire lasers were also developed that could directly emit few-cycle pulses and octave-spanning spectra (102–104).

Although Ti:sapphire has proven to be a reliable approach in some frequency comb systems (104), the most widespread and mature frequency comb technology is now realized with mode-locked lasers using erbium-doped fiber as a gain medium (105). These leverage the robustness and fiber-integrated components provided by the telecommunications industry in the 1550-nm region of the spectrum (106–111). Er: fiber frequency combs employ solid-core nonlinear fibers to generate octave-span spectra; these comb systems, including gain fiber, pump lasers, amplifiers, and nonlinear fibers, can be entirely spliced together, making them extremely robust (112). Such frequency combs are commercially available from several companies, run autonomously in spectroscopy and metrology applications, and have even been operated on board a sounding rocket (113). Lasers using Yb- and Tm-doped fibers, as well as other solid state materials, have led to an expanding palette of frequency comb spectra (114, 115). Additionally, nonlinear optical processes have pushed the extent of frequency combs across the terahertz (THz) (116, 117) and mid-infrared (MIR) (118–122) domains and all the way into the extreme ultraviolet (XUV) (123–126) for a wide range of sensing, clock, and spectroscopic applications.

#### Electro-optic frequency combs

An early approach to generate a frequency comb employed an electro-optical (EO) modulator driven by a microwave signal to impose a grid of sidebands on a continuous-wave laser (127). Building on this core EO technological piece,

in 1993 Motonobu Kourogi and co-workers introduced a very efficient modulator-based comb generator (85). The idea was to place the modulator inside an optical resonator and drive it with a microwave signal that matched the optical resonator mode spacing. As a result, the generated sidebands are resonantly enhanced and generate sidebands themselves (Fig. 5B). Although the input seed laser frequency might not be absolutely stable, these modulator-based comb generators could be used like a ruler to measure optical intervals of a few THz, limited ultimately by dispersion inside the resonant optical cavity (128). EO combs became an attractive part of the Hänsch interval division technique (Fig. 2, C to E) once the gap between successive subharmonics was reduced down a value on the order of the EO comb bandwidth (27). Efforts to increase the bandwidth of EO combs included spectral broadening in an optical fiber outside the EO cavity (129), or the introduction of parametric gain inside the EO cavity (130), and recent advances in integrated lithium-niobate waveguides promise still broader bandwidths (131) along the lines of Kourogi’s original modulator-in-a-cavity design.

Although mode-locked laser combs and their octave-spanning frequency spectra supplanted EO combs, the simplicity and deterministic nature of the EO comb remained attractive. And thanks to improved lithium niobate waveguide modulators coming from the telecommunications industry, a different approach to EO combs reemerged around 2010 (132–134). Instead of placing the EO comb inside an optical cavity, modulators can be cascaded one after another, and with appropriately phased microwave drive, each modulator adds additional comb lines. This results in a broad bandwidth and spectrally flat frequency comb that can be compressed into a short pulse for additional nonlinear spectral broadening. However, owing to the multiplicative nature of this comb generator, the microwave phase noise can ultimately grow to overwhelm the comb teeth themselves. Recently, this problem was resolved with the introduction of an optical cavity filter, which resulted in an octave-span EO comb for which  $f_0$  could be measured (135). Efficient spectral broadening using nanophotonic silicon nitride waveguides, such as shown in Fig. 5F, combined with techniques to further reduce the noise of the microwave source have now resulted in an EO comb with noise that is comparable to that of mode-locked laser combs (136).

#### Microresonator frequency combs

A third approach to the formation of frequency combs has attracted interest because it offers the prospect of miniature comb systems integrated on a semiconductor chip (137). Often called microcombs, these devices rely on access

to the Kerr nonlinearity at milliwatt power levels through resonant enhancement of light in whispering-gallery microresonators (138–140) or in ring-like resonators as shown in Fig. 5C (141, 142). Key to their operation is the confinement of the input single-frequency laser light in a resonator mode with a cross-section of  $\approx 1 \mu\text{m}^2$  that has very low propagation loss, with material and dielectric-interface-dependent quality factors ranging from  $Q \approx 10^6$  up to nearly  $10^{11}$  being achieved. Under these conditions, milliwatts (or less) of input power are resonantly enhanced to as high as kilowatt levels, so that two sidebands are spontaneously generated with equal spacing about the pump frequency through parametric oscillation mediated by the Kerr nonlinearity (143, 144). This process can cascade through four-wave mixing such that additional sidebands are generated (143), and in 2007 it was shown to lead to a frequency comb (145). Developments related to solitons in optical fiber cavities (146, 147) combined with a deeper understand-

ing of cascaded combs eventually led to operational modes where isolated solitons could be generated in microresonators (148–152). As with mode-locked lasers described above, a soliton pulse that propagates with unchanging shape around the cavity is the basis of a frequency comb.

Critical to the generation of solitons in microresonators is the control of the dispersion that the pulse experiences while traveling around the cavity. Here the lithographic control offered by modern fabrication techniques permits adjustment of geometric dispersion through nanometer-scale dimensional changes to the waveguide cross section (153, 154). Most notably, this has led to microresonator designs that directly generate solitons with octave-spanning spectra (142, 155). An example of such a resonator made from silicon nitride is shown in Fig. 5G, and its resulting comb spectrum with 1-THz mode spacing is shown in Fig. 5C. Other microresonator materials, such as aluminum nitride (156), lithium niobate

(157), and III-V semiconductors (158), offer both third- and second-order nonlinearities that could potentially be used to both generate octave-span combs and then double the frequency of the long-wavelength parts for self-referencing.

There has been tremendous progress with microcomb system demonstrations, including optical frequency synthesis (159) and optical clocks (160, 161). But there is still much work to be done before the full integration potential of microcombs is realized, as most still require off-chip lasers, amplifiers, or other optical fiber components. Nonetheless, repetition rates in the 10- to 100-GHz range make microcombs attractive for applications, including astronomical spectrograph calibration (162, 163) and optical communications (164). Moreover, the high repetition rates can be advantageous in dual-comb measurements where high-speed acquisition is desirable, as shown in recent spectroscopy (165, 166) and light detection and ranging (LIDAR) (167, 168) demonstrations.

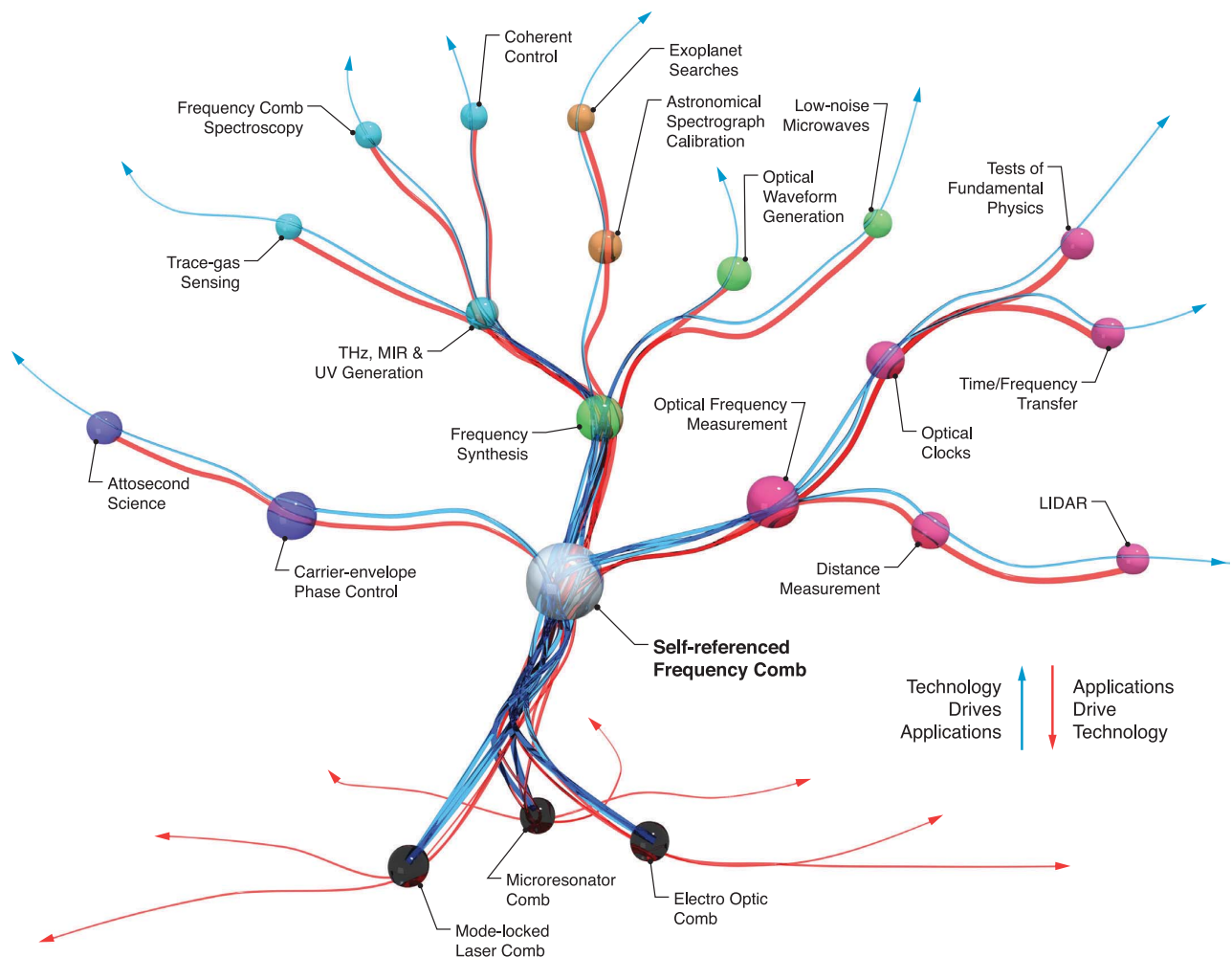


**Fig. 6. The frequency comb evolutionary tree reenvisioned.** Technology drives new applications, and applications feed the growth of new technologies.

## The continuously evolving optical frequency comb

Optical frequency combs were originally developed to solve the problem of measuring and counting optical frequencies in terms of the SI cesium definition. As we have described, this was of critical importance for applications in precision spectroscopy and time and frequency metrology. And though spectacularly successful in that role, 20 years ago it was impossible to foresee the range of applications beyond metrology, spectroscopy, and clocks for which frequency combs are now being used. Indeed, one of the most surprising developments of optical frequency combs has been the diversity of applications that they have found and opened, as well as the intertwined technologies they have employed (Fig. 6). The symbiotic relationship between applications and technologies can be depicted as a kind of living and evolving tree (114), where new applications sprout upward as technological roots spread downward. The branches and roots find at their center the key aspect of self-referencing, which is the distinguishing feature of a frequency comb that coherently connects the optical and electrical realms.

The scientific depth and range of the technological roots that produce frequency combs have also evolved substantially, with several surprising innovations that rapidly advanced frequency comb capabilities. Far before the first self-referenced Ti:sapphire mode-locked lasers, nascent frequency comb spectroscopy was performed with a synchronously pumped dye laser that contained just six to eight frequency modes and a bandwidth that could only enable difference frequency measurements across a 1-GHz gap (169). This was expanded to the THz range with the introduction of EO comb technology in the 1990s. However, that did not forecast the serendipitous meeting of the Ti:sapphire laser with nonlinear fibers that led to the immediate expansion of frequency combs to hundreds of terahertz and the octave span required for self-referencing (32–34). Twenty years later, this self-referencing is now a routine part of the clockwork of the Er: fiber frequency combs that run autonomously as the most robust and widely used comb technology (111).

Nanoscale waveguide technology and nonlinear optics, that first appeared in the microstructure fiber, is another technology with significant evolutionary impact on frequency comb generation. Microresonator frequency combs (137, 145, 152) not only provide a comb-generating mechanism different from that of mode-locked lasers, but they can be built at wafer scale in a manner analogous to the fabrication of integrated electronic circuits. This is a first step along the path toward future self-referenced frequency combs that

could be fully integrated on a chip in a robust package, perhaps along with other capabilities of advanced photonic integrated circuits (170). The same nanoscale waveguide fabrication also opens new opportunities by providing ultra-efficient nonlinear spectral broadening. For Er: fiber combs, this appears to be critical for applications such as space flight that would demand low electrical power (171). And for the older EO comb technology, this has made octave-span spectra at 10-GHz rates possible with a factor of 10 less power (136), which drives applications such as exoplanet astrophysics with a continuously running calibration comb (67). Thus, the connection between technology, applications, and science continues to grow.

In hindsight, perhaps the spread and interlacing of applications and technologies of Fig. 6 are a natural outcome, given the core synthesis and connectivity function of the frequency comb. And looking forward to the coming decades, we can only speculate on the new applications and technological roots that might emerge. It seems likely that as the technology becomes more integrated and tightly interfaced with applications, the boundary between electronics and optics will be further blurred, and the uniting aspects of the frequency comb on the electromagnetic spectrum will be more fully realized for advancing science.

## REFERENCES AND NOTES

- H. Hertz, *Untersuchungen über die Ausbreitung der elektrischen Kraft* (Johann Ambrosius Baath, Leipzig, 1894).
- T. W. Hänsch, Nobel lecture: Passion for precision. *Rev. Mod. Phys.* **78**, 1297–1309 (2006). doi: [10.1103/RevModPhys.78.1297](https://doi.org/10.1103/RevModPhys.78.1297)
- J. L. Hall, Nobel lecture: Defining and measuring optical frequencies. *Rev. Mod. Phys.* **78**, 1279–1295 (2006). doi: [10.1103/RevModPhys.78.1279](https://doi.org/10.1103/RevModPhys.78.1279); pmid: [17086589](https://pubmed.ncbi.nlm.nih.gov/17086589/)
- J. H. Bryant, The first century of microwaves-1886 to 1986. *IEEE Trans. Microw. Theory Tech.* **36**, 830–858 (1988). doi: [10.1109/22.3602](https://doi.org/10.1109/22.3602)
- J. C. Maxwell, *A Treatise on Electricity and Magnetism* (Macmillan and Co, London, 1873).
- E. H. Armstrong, Some recent developments in the audion receiver. *Proc. Inst. Radio Eng.* **3**, 215 (1915).
- J. P. Gordon, H. J. Zeiger, C. H. Townes, The maser—New type of microwave amplifier, frequency standard, and spectrometer. *Phys. Rev.* **99**, 1264–1274 (1955). doi: [10.1103/PhysRev.99.1264](https://doi.org/10.1103/PhysRev.99.1264)
- A. L. Schawlow, C. H. Townes, Infrared and optical masers. *Phys. Rev.* **112**, 1940–1949 (1958). doi: [10.1103/PhysRev.112.1940](https://doi.org/10.1103/PhysRev.112.1940)
- T. H. Maiman, R. H. Hoskins, I. J. D'Haenens, C. K. Asawa, V. Evtuhov, Stimulated optical emission in fluorescent solids. ii. spectroscopy and stimulated emission in ruby. *Phys. Rev.* **123**, 1151–1157 (1961). doi: [10.1103/PhysRev.123.1151](https://doi.org/10.1103/PhysRev.123.1151)
- A. Javan, W. R. Bennett, D. R. Herriott, Population inversion and continuous optical maser oscillation in a gas discharge containing a he-ne mixture. *Phys. Rev. Lett.* **6**, 106–110 (1961). doi: [10.1103/PhysRevLett.6.106](https://doi.org/10.1103/PhysRevLett.6.106)
- A. Javan, E. A. Ballik, W. L. Bond, Frequency characteristics of a continuous-wave He-Ne optical maser. *J. Opt. Soc. Am.* **52**, 96 (1962). doi: [10.1364/JOSA.52.000096](https://doi.org/10.1364/JOSA.52.000096)
- L. O. Hocker, A. Javan, D. R. Rao, L. Frenkel, T. Sullivan, Absolute frequency measurement and spectroscopy of gas laser transitions in the far infrared. *Appl. Phys. Lett.* **10**, 147–149 (1967). doi: [10.1063/1.1754887](https://doi.org/10.1063/1.1754887)
- K. Evenson, J. Wells, F. Petersen, B. Danielson, G. Day, Accurate frequencies of molecular transitions used in laser stabilization: The 3.39- $\mu\text{m}$  transition in  $\text{CH}_4$  and the 9.33- and 10.18- $\mu\text{m}$  transitions in  $\text{CO}_2$ . *Appl. Phys. Lett.* **22**, 192–195 (1973). doi: [10.1063/1.1654607](https://doi.org/10.1063/1.1654607)
- V. P. Chebotayev *et al.*, Development of an optical time scale. *Appl. Phys. B* **29**, 63–65 (1982). doi: [10.1007/BF00694370](https://doi.org/10.1007/BF00694370)
- H. Schnatz, B. Lipphardt, J. Helmcke, F. Riehle, G. Zinner, First phase-coherent frequency measurement of visible radiation. *Phys. Rev. Lett.* **76**, 18–21 (1996). doi: [10.1103/PhysRevLett.76.18](https://doi.org/10.1103/PhysRevLett.76.18); pmid: [10060423](https://pubmed.ncbi.nlm.nih.gov/10060423/)
- D. J. Wineland, Laser-to-microwave frequency division using synchrotron radiation. *J. Appl. Phys.* **50**, 2528–2532 (1979). doi: [10.1063/1.326249](https://doi.org/10.1063/1.326249)
- V. P. Chebotayev, Synchronization of Quantum Transitions. *JETP Lett.* **49**, 489 (1989).
- K. M. Evenson *et al.*, Speed of light from direct frequency and wavelength measurements of the methane-stabilized laser. *Phys. Rev. Lett.* **29**, 1346–1349 (1972). doi: [10.1103/PhysRevLett.29.1346](https://doi.org/10.1103/PhysRevLett.29.1346)
- P. Giacomo, News from the BIPM: Some Changes in the SI. *IEEE Trans. Instrum. Meas.* **IM-34**, 116–117 (1985). doi: [10.1109/TIM.1985.4315282](https://doi.org/10.1109/TIM.1985.4315282)
- M. Stock, R. Davis, E. de Mirandés, M. J. T. Milton, E. de Mirandés, The revision of the SI—The result of three decades of progress in metrology. *Metrologia* **56**, 022001 (2019). doi: [10.1088/1681-7575/ab0013](https://doi.org/10.1088/1681-7575/ab0013)
- R. L. Barger, J. L. Hall, Pressure shift and broadening of methane line at 3.39  $\mu\text{m}$ . *Phys. Rev. Lett.* **22**, 4–8 (1969). doi: [10.1103/PhysRevLett.22.4](https://doi.org/10.1103/PhysRevLett.22.4)
- S. N. Bagayev *et al.*, A tunable laser at  $\lambda = 3.39 \mu\text{m}$  with line width of 7 Hz used in investigating a hyperfine structure of the  $\text{F}_2^{(2)}$  line of methane. *Appl. Phys.* **13**, 291–297 (1977). doi: [10.1007/BF00882895](https://doi.org/10.1007/BF00882895)
- B. de Beauvoir *et al.*, Absolute frequency measurement of the  $2S - 8S/D$ . *Phys. Rev. Lett.* **78**, 440–443 (1997). doi: [10.1103/PhysRevLett.78.440](https://doi.org/10.1103/PhysRevLett.78.440)
- T. Udem *et al.*, Phase-Coherent Measurement of the Hydrogen  $1S-2S$  Transition Frequency with an Optical Frequency Interval Divider Chain. *Phys. Rev. Lett.* **79**, 2646–2649 (1997). doi: [10.1103/PhysRevLett.79.2646](https://doi.org/10.1103/PhysRevLett.79.2646)
- T. W. Hänsch, *The Hydrogen Atom*, G. F. Bassani, M. Inguscio, T. W. Hänsch, eds. (Springer Berlin Heidelberg, Berlin, Heidelberg, 1989), pp. 93–102.
- T. Udem, Phasenkohärente optische Frequenzmessungen am Wasserstoffatom. Bestimmung der Rydberg-Konstanten und der  $1S$  Lamb-Verschiebung, thesis, Ludwig-Maximilians-Universität München, Germany (1997).
- K. Nakagawa, M. Kourogi, M. Ohtsu, Proposal of a frequency-synthesis chain between the microwave and optical frequencies of the Ca intercombination line at 657 nm using diode lasers. *Appl. Phys. B* **57**, 425–430 (1993). doi: [10.1007/BF00357386](https://doi.org/10.1007/BF00357386)
- J. N. Eckstein, High resolution spectroscopy using multiple coherent interactions, Ph.D. thesis, Stanford University (1978).
- A. I. Ferguson, J. N. Eckstein, T. W. Hänsch, Polarization spectroscopy with ultrashort light pulses. *Appl. Phys. (Berl.)* **18**, 257–260 (1979). doi: [10.1007/BF00885511](https://doi.org/10.1007/BF00885511)
- T. Udem, R. Holzwarth, T. W. Hänsch, Optical frequency metrology. *Nature* **416**, 233–237 (2002). doi: [10.1038/416233a](https://doi.org/10.1038/416233a); pmid: [11894107](https://pubmed.ncbi.nlm.nih.gov/11894107/)
- J. Reichert, R. Holzwarth, T. Udem, T. W. Hänsch, Measuring the frequency of light with mode-locked lasers. *Opt. Commun.* **172**, 59–68 (1999). doi: [10.1016/S0030-4018\(99\)00491-5](https://doi.org/10.1016/S0030-4018(99)00491-5)
- D. J. Jones *et al.*, Carrier-envelope phase control of femtosecond mode-locked lasers and direct optical frequency synthesis. *Science* **288**, 635–640 (2000). doi: [10.1126/science.288.5466.635](https://doi.org/10.1126/science.288.5466.635); pmid: [10784441](https://pubmed.ncbi.nlm.nih.gov/10784441/)
- S. A. Diddams *et al.*, Direct link between microwave and optical frequencies with a 300 THz femtosecond laser comb. *Phys. Rev. Lett.* **84**, 5102–5105 (2000). doi: [10.1103/PhysRevLett.84.5102](https://doi.org/10.1103/PhysRevLett.84.5102); pmid: [10990877](https://pubmed.ncbi.nlm.nih.gov/10990877/)
- R. Holzwarth *et al.*, Optical frequency synthesizer for precision spectroscopy. *Phys. Rev. Lett.* **85**, 2264–2267 (2000). doi: [10.1103/PhysRevLett.85.2264](https://doi.org/10.1103/PhysRevLett.85.2264); pmid: [10977987](https://pubmed.ncbi.nlm.nih.gov/10977987/)
- T. Udem *et al.*, Absolute frequency measurements of the  $\text{Hg}^+$  and Ca optical clock transitions with a femtosecond laser  $\text{Hg}^+$ . *Phys. Rev. Lett.* **86**, 4996–4999 (2001). doi: [10.1103/PhysRevLett.86.4996](https://doi.org/10.1103/PhysRevLett.86.4996); pmid: [11384404](https://pubmed.ncbi.nlm.nih.gov/11384404/)
- J. Ye *et al.*, Accuracy comparison of absolute optical frequency measurement between harmonic-generation synthesis and a frequency-division femtosecond comb. *Phys. Rev. Lett.* **85**, 3797–3800 (2000). doi: [10.1103/PhysRevLett.85.3797](https://doi.org/10.1103/PhysRevLett.85.3797); pmid: [11041930](https://pubmed.ncbi.nlm.nih.gov/11041930/)
- S. Bize *et al.*, Testing the stability of fundamental constants with the  $^{199}\text{Hg}^+$  single-ion optical clock  $^{199}\text{Hg}^+$ . *Phys. Rev. Lett.* **90**, 150802 (2003). doi: [10.1103/PhysRevLett.90.150802](https://doi.org/10.1103/PhysRevLett.90.150802); pmid: [12732024](https://pubmed.ncbi.nlm.nih.gov/12732024/)



38. M. Fischer *et al.*, New limits on the drift of fundamental constants from laboratory measurements. *Phys. Rev. Lett.* **92**, 230802 (2004). doi: [10.1103/PhysRevLett.92.230802](https://doi.org/10.1103/PhysRevLett.92.230802); pmid: [15245149](https://pubmed.ncbi.nlm.nih.gov/15245149/)
39. T. M. Fortier *et al.*, Precision atomic spectroscopy for improved limits on variation of the fine structure constant and local position invariance. *Phys. Rev. Lett.* **98**, 070801 (2007). doi: [10.1103/PhysRevLett.98.070801](https://doi.org/10.1103/PhysRevLett.98.070801); pmid: [17359009](https://pubmed.ncbi.nlm.nih.gov/17359009/)
40. R. Holzwarth *et al.*, Absolute frequency measurement of iodine lines with a femtosecond optical synthesizer. *Appl. Phys. B* **73**, 269–271 (2001). doi: [10.1007/s003400100633](https://doi.org/10.1007/s003400100633)
41. V. Gerginov, C. E. Tanner, S. Diddams, A. Bartels, L. Hollberg, Optical frequency measurements of  $6s^2\ ^1S_{1/2} - 6p^2\ ^3P_{3/2}$  transition in a  $^{133}\text{Cs}$  atomic beam using a femtosecond laser frequency comb. *Phys. Rev. A* **70**, 042505 (2004). doi: [10.1103/PhysRevA.70.042505](https://doi.org/10.1103/PhysRevA.70.042505)
42. F.-L. Hong *et al.*, Frequency measurements and hyperfine structure of the  $r(85)33\text{-O}$  transition of molecular iodine with a femtosecond optical comb. *J. Opt. Soc. Am. B* **21**, 88 (2004). doi: [10.1364/JOSAB.21.000088](https://doi.org/10.1364/JOSAB.21.000088)
43. A. Marian, M. C. Stowe, J. R. Lawall, D. Felinto, J. Ye, United time-frequency spectroscopy for dynamics and global transport. *Science* **306**, 2063–2068 (2004). doi: [10.1126/science.1105660](https://doi.org/10.1126/science.1105660); pmid: [15550622](https://pubmed.ncbi.nlm.nih.gov/15550622/)
44. V. Gerginov, C. E. Tanner, S. A. Diddams, A. Bartels, L. Hollberg, High-resolution spectroscopy with a femtosecond laser frequency comb. *Opt. Lett.* **30**, 1734–1736 (2005). doi: [10.1364/OL.30.001734](https://doi.org/10.1364/OL.30.001734); pmid: [16075554](https://pubmed.ncbi.nlm.nih.gov/16075554/)
45. E. Baumann *et al.*, Spectroscopy of the methane  $\nu_3$  band with an accurate midinfrared coherent dual-comb spectrometer. *Phys. Rev. A* **84**, 062513 (2011). doi: [10.1103/PhysRevA.84.062513](https://doi.org/10.1103/PhysRevA.84.062513)
46. A. M. Zolot *et al.*, Broad-band frequency references in the near-infrared: Accurate dual comb spectroscopy of methane and acetylene. *J. Quant. Spectrosc. Radiat. Transf.* **118**, 26–39 (2013). doi: [10.1016/j.jqsrt.2012.11.024](https://doi.org/10.1016/j.jqsrt.2012.11.024)
47. M. J. Thorpe, K. D. Moll, R. J. Jones, B. Safdi, J. Ye, Broadband cavity ringdown spectroscopy for sensitive and rapid molecular detection. *Science* **311**, 1595–1599 (2006). doi: [10.1126/science.1123921](https://doi.org/10.1126/science.1123921); pmid: [16543457](https://pubmed.ncbi.nlm.nih.gov/16543457/)
48. B. Bernhardt *et al.*, Cavity-enhanced dual-comb spectroscopy. *Nat. Photonics* **4**, 55–57 (2010). doi: [10.1038/nphoton.2009.217](https://doi.org/10.1038/nphoton.2009.217)
49. S. A. Diddams, L. Hollberg, V. Mbele, Molecular fingerprinting with the resolved modes of a femtosecond laser frequency comb. *Nature* **445**, 627–630 (2007). doi: [10.1038/nature05524](https://doi.org/10.1038/nature05524); pmid: [17287805](https://pubmed.ncbi.nlm.nih.gov/17287805/)
50. C. Gohle, B. Stein, A. Schliesser, T. Udem, T. W. Hänsch, Frequency comb Vernier spectroscopy for broadband, high-resolution, high-sensitivity absorption and dispersion spectra. *Phys. Rev. Lett.* **99**, 263902 (2007). doi: [10.1103/PhysRevLett.99.263902](https://doi.org/10.1103/PhysRevLett.99.263902); pmid: [18233578](https://pubmed.ncbi.nlm.nih.gov/18233578/)
51. S. Schiller, Spectrometry with frequency combs. *Opt. Lett.* **27**, 766–768 (2002). doi: [10.1364/OL.27.000766](https://doi.org/10.1364/OL.27.000766); pmid: [18007926](https://pubmed.ncbi.nlm.nih.gov/18007926/)
52. F. Keilmann, C. Gohle, R. Holzwarth, Time-domain mid-infrared frequency-comb spectrometer. *Opt. Lett.* **29**, 1542–1544 (2004). doi: [10.1364/OL.29.001542](https://doi.org/10.1364/OL.29.001542); pmid: [15259740](https://pubmed.ncbi.nlm.nih.gov/15259740/)
53. I. Coddington, W. C. Swann, N. R. Newbury, Coherent multiheterodyne spectroscopy using stabilized optical frequency combs. *Phys. Rev. Lett.* **100**, 013902 (2008). doi: [10.1103/PhysRevLett.100.013902](https://doi.org/10.1103/PhysRevLett.100.013902); pmid: [18232764](https://pubmed.ncbi.nlm.nih.gov/18232764/)
54. J. Roy, J.-D. Deschênes, S. Potvin, J. Genest, Continuous real-time correction and averaging for frequency comb interferometry. *Opt. Express* **20**, 21932–21939 (2012). doi: [10.1364/OE.20.021932](https://doi.org/10.1364/OE.20.021932); pmid: [23037343](https://pubmed.ncbi.nlm.nih.gov/23037343/)
55. T. Ideguchi *et al.*, Coherent Raman spectro-imaging with laser frequency combs. *Nature* **502**, 355–358 (2013). doi: [10.1038/nature12607](https://doi.org/10.1038/nature12607); pmid: [24132293](https://pubmed.ncbi.nlm.nih.gov/24132293/)
56. F. R. Giorgetta *et al.*, Broadband phase spectroscopy over turbulent air paths. *Phys. Rev. Lett.* **115**, 103901 (2015). doi: [10.1103/PhysRevLett.115.103901](https://doi.org/10.1103/PhysRevLett.115.103901); pmid: [26382677](https://pubmed.ncbi.nlm.nih.gov/26382677/)
57. I. Coddington, N. Newbury, W. Swann, Dual-comb spectroscopy. *Optica* **3**, 414 (2016). doi: [10.1364/OPTICA.3.000414](https://doi.org/10.1364/OPTICA.3.000414)
58. K. C. Cossel *et al.*, Gas-phase broadband spectroscopy using active sources: Progress, status, and applications. *J. Opt. Soc. Am. B* **34**, 104–129 (2017). doi: [10.1364/JOSAB.34.000104](https://doi.org/10.1364/JOSAB.34.000104); pmid: [28630530](https://pubmed.ncbi.nlm.nih.gov/28630530/)
59. N. Picqué, T. W. Hänsch, Frequency comb spectroscopy. *Nat. Photonics* **13**, 146–157 (2019). doi: [10.1038/s41566-018-0347-5](https://doi.org/10.1038/s41566-018-0347-5)
60. T. Steinmetz *et al.*, Laser frequency combs for astronomical observations. *Science* **321**, 1335–1337 (2008). doi: [10.1126/science.1161030](https://doi.org/10.1126/science.1161030); pmid: [18772434](https://pubmed.ncbi.nlm.nih.gov/18772434/)
61. A. J. Metcalf *et al.*, Stellar spectroscopy in the near-infrared with a laser frequency comb. *Optica* **6**, 233 (2019). doi: [10.1364/OPTICA.6.000233](https://doi.org/10.1364/OPTICA.6.000233)
62. R. A. Probst *et al.*, A crucial test for astronomical spectrograph calibration with frequency combs. *Nature Astronomy* (2020).
63. S. A. Diddams *et al.*, An optical clock based on a single trapped  $^{199}\text{Hg}^+$  ion. *Science* **293**, 825–828 (2001). doi: [10.1126/science.1061171](https://doi.org/10.1126/science.1061171); pmid: [11452082](https://pubmed.ncbi.nlm.nih.gov/11452082/)
64. J. Ye, L. S. Ma, J. L. Hall, Molecular iodine clock. *Phys. Rev. Lett.* **87**, 270801 (2001). doi: [10.1103/PhysRevLett.87.270801](https://doi.org/10.1103/PhysRevLett.87.270801); pmid: [11800866](https://pubmed.ncbi.nlm.nih.gov/11800866/)
65. D. Wineland, H. Dehmelt, Proposed  $10^{14}$   $\Delta\nu/\nu$  laser fluorescence spectroscopy on  $\text{Ti}^+$  mono-ion oscillator. *Bull. Am. Phys. Soc.* **20**, 637 (1975).
66. T. W. Hänsch, A. L. Schawlow, Cooling of gases by laser radiation. *Opt. Commun.* **13**, 68–69 (1975). doi: [10.1016/0030-4018\(75\)90159-5](https://doi.org/10.1016/0030-4018(75)90159-5)
67. C. W. Chou, D. B. Hume, M. J. Thorpe, D. J. Wineland, T. Rosenband, Quantum coherence between two atoms beyond  $Q = 10^{15}$ . *Phys. Rev. Lett.* **106**, 160801 (2011). doi: [10.1103/PhysRevLett.106.160801](https://doi.org/10.1103/PhysRevLett.106.160801); pmid: [21599347](https://pubmed.ncbi.nlm.nih.gov/21599347/)
68. B. C. Young, F. C. Cruz, W. M. Itano, J. C. Bergquist, Visible lasers with subhertz linewidths. *Phys. Rev. Lett.* **82**, 3799–3802 (1999). doi: [10.1103/PhysRevLett.82.3799](https://doi.org/10.1103/PhysRevLett.82.3799)
69. M. Notcutt, L.-S. Ma, J. Ye, J. L. Hall, Simple and compact 1-Hz laser system via an improved mounting configuration of a reference cavity. *Opt. Lett.* **30**, 1815–1817 (2005). doi: [10.1364/OL.30.001815](https://doi.org/10.1364/OL.30.001815); pmid: [16092355](https://pubmed.ncbi.nlm.nih.gov/16092355/)
70. K. Numata, A. Kemery, J. Camp, Thermal-noise limit in the frequency stabilization of lasers with rigid cavities. *Phys. Rev. Lett.* **93**, 250602 (2004). doi: [10.1103/PhysRevLett.93.250602](https://doi.org/10.1103/PhysRevLett.93.250602); pmid: [15697887](https://pubmed.ncbi.nlm.nih.gov/15697887/)
71. J. M. Robinson *et al.*, Crystalline optical cavity at 4 K with thermal-noise-limited instability and ultralow drift. *Optica* **6**, 240 (2019). doi: [10.1364/OPTICA.6.000240](https://doi.org/10.1364/OPTICA.6.000240)
72. T. L. Nicholson *et al.*, Systematic evaluation of an atomic clock at  $2 \times 10^{-18}$  total uncertainty. *Nat. Commun.* **6**, 6896 (2015). doi: [10.1038/ncomms7896](https://doi.org/10.1038/ncomms7896); pmid: [25898253](https://pubmed.ncbi.nlm.nih.gov/25898253/)
73. W. F. McGrew *et al.*, Atomic clock performance enabling geodesy below the centimetre level. *Nature* **564**, 87–90 (2018). doi: [10.1038/s41586-018-0738-2](https://doi.org/10.1038/s41586-018-0738-2); pmid: [30487601](https://pubmed.ncbi.nlm.nih.gov/30487601/)
74. S. M. Brewer *et al.*,  $^{27}\text{Al}^+$  Quantum-logic clock with a systematic uncertainty below  $10^{-18}$ . *Phys. Rev. Lett.* **123**, 033201 (2019). doi: [10.1103/PhysRevLett.123.033201](https://doi.org/10.1103/PhysRevLett.123.033201); pmid: [31386450](https://pubmed.ncbi.nlm.nih.gov/31386450/)
75. I. Ushijima, M. Takamoto, M. Das, T. Ohkubo, H. Katori, Cryogenic optical lattice clocks. *Nat. Photonics* **9**, 185–189 (2015). doi: [10.1038/nphoton.2015.5](https://doi.org/10.1038/nphoton.2015.5)
76. N. Huntemann, C. Sanner, B. Lipphardt, C. Tamm, E. Peik, Single-ion atomic clock with  $3 \times 10^{-18}$  systematic uncertainty. *Phys. Rev. Lett.* **116**, 063001 (2016). doi: [10.1103/PhysRevLett.116.063001](https://doi.org/10.1103/PhysRevLett.116.063001); pmid: [26918984](https://pubmed.ncbi.nlm.nih.gov/26918984/)
77. T. Fortier *et al.*, Generation of ultrastable microwaves via optical frequency division. *Nat. Photonics* **5**, 425–429 (2011). doi: [10.1038/nphoton.2011.121](https://doi.org/10.1038/nphoton.2011.121)
78. X. Xie *et al.*, Photonic microwave signals with zeptosecond-level absolute timing noise. *Nat. Photonics* **11**, 44–47 (2017). doi: [10.1038/nphoton.2016.215](https://doi.org/10.1038/nphoton.2016.215)
79. C. Grebing *et al.*, Realization of a timescale with an accurate optical lattice clock. *Optica* **3**, 563 (2016). doi: [10.1364/OPTICA.3.000563](https://doi.org/10.1364/OPTICA.3.000563)
80. H. Hachisu, F. Nakagawa, Y. Hanado, T. Ido, Months-long real-time generation of a time scale based on an optical clock. *Sci. Rep.* **8**, 4243 (2018). doi: [10.1038/s41598-018-22423-5](https://doi.org/10.1038/s41598-018-22423-5); pmid: [29523792](https://pubmed.ncbi.nlm.nih.gov/29523792/)
81. J. Yao *et al.*, Optical-clock-based time scale. *Phys. Rev. Appl.* **12**, 044069 (2019). doi: [10.1103/PhysRevApplied.12.044069](https://doi.org/10.1103/PhysRevApplied.12.044069); pmid: [31702265](https://pubmed.ncbi.nlm.nih.gov/31702265/)
82. W. R. Milner *et al.*, Demonstration of a timescale based on a stable optical carrier. *Phys. Rev. Lett.* **123**, 173201 (2019). doi: [10.1103/PhysRevLett.123.173201](https://doi.org/10.1103/PhysRevLett.123.173201); pmid: [31702265](https://pubmed.ncbi.nlm.nih.gov/31702265/)
83. H. Margolis, Timekeepers of the future. *Nat. Phys.* **10**, 82–83 (2014). doi: [10.1038/nphys2834](https://doi.org/10.1038/nphys2834)
84. F. Riehle, P. Gill, F. Arias, L. Robertson, The CIPM list of recommended frequency standard values: Guidelines and procedures. *Metrologia* **55**, 188–200 (2018). doi: [10.1088/1681-7575/aaa302](https://doi.org/10.1088/1681-7575/aaa302)
85. M. Kourogi, N. Ken'ichi, M. Ohtsu, Wide-Span Optical Frequency Comb Generator for Accurate Optical Frequency Difference Measurement. *IEEE J. Quantum Electron.* **29**, 2693–2701 (1993). doi: [10.1109/3.250392](https://doi.org/10.1109/3.250392)
86. J. Stenger, H. Schnatz, C. Tamm, H. R. Telle, Ultraprecise measurement of optical frequency ratios. *Phys. Rev. Lett.* **88**, 073601 (2002). doi: [10.1103/PhysRevLett.88.073601](https://doi.org/10.1103/PhysRevLett.88.073601); pmid: [11863895](https://pubmed.ncbi.nlm.nih.gov/11863895/)
87. T. Rosenband *et al.*, Frequency ratio of  $\text{Al}^+$  and  $\text{Hg}^+$  single-ion optical clocks; metrology at the 17th decimal place. *Science* **319**, 1808–1812 (2008). pmid: [18323415](https://pubmed.ncbi.nlm.nih.gov/18323415/)
88. R. M. Godun *et al.*, Frequency ratio of two optical clock transitions in  $^{171}\text{Yb}^+$  and constraints on the time variation of fundamental constants. *Phys. Rev. Lett.* **113**, 210801 (2014). doi: [10.1103/PhysRevLett.113.210801](https://doi.org/10.1103/PhysRevLett.113.210801); pmid: [25479482](https://pubmed.ncbi.nlm.nih.gov/25479482/)
89. P. Woisio *et al.*, New bounds on dark matter coupling from a global network of optical atomic clocks. *Sci. Adv.* **4**, eaau4869 (2018). doi: [10.1126/sciadv.aau4869](https://doi.org/10.1126/sciadv.aau4869); pmid: [30539146](https://pubmed.ncbi.nlm.nih.gov/30539146/)
90. M. S. Safronova *et al.*, Search for new physics with atoms and molecules. *Rev. Mod. Phys.* **90**, 025008 (2018). doi: [10.1103/RevModPhys.90.025008](https://doi.org/10.1103/RevModPhys.90.025008)
91. F. R. Giorgetta *et al.*, Optical two-way time and frequency transfer over free space. *Nat. Photonics* **7**, 434–438 (2013). doi: [10.1038/nphoton.2013.69](https://doi.org/10.1038/nphoton.2013.69)
92. I. Coddington, W. C. Swann, L. Nenadovic, N. R. Newbury, Rapid and precise absolute distance measurements at long range. *Nat. Photonics* **3**, 351–356 (2009). doi: [10.1038/nphoton.2009.94](https://doi.org/10.1038/nphoton.2009.94)
93. L. Xu *et al.*, Route to phase control of ultrashort light pulses. *Opt. Lett.* **21**, 2008–2010 (1996). doi: [10.1364/OL.21.002008](https://doi.org/10.1364/OL.21.002008); pmid: [19881875](https://pubmed.ncbi.nlm.nih.gov/19881875/)
94. H. R. Telle *et al.*, Carrier-envelope offset phase control: A novel concept for absolute optical frequency measurement and ultrashort pulse generation. *Appl. Phys. B* **69**, 327–332 (1999). doi: [10.1007/s003400050813](https://doi.org/10.1007/s003400050813)
95. J. K. Ranka, R. S. Windeler, A. J. Stentz, *Technical Digest of Papers Presented at the Conference on Lasers and Electro-Optics. CLEO '99* (IEEE catalog no.99CH37013) (1999), pp. CPD8/1–CPD8/2.
96. W. J. Wadsworth *et al.*, Soliton effects in photonic crystal fibers at 850 nm. *Electron. Lett.* **36**, 53 (2000). doi: [10.1049/el:20000134](https://doi.org/10.1049/el:20000134)
97. J. K. Ranka, R. S. Windeler, A. J. Stentz, Visible continuum generation in air-silica microstructure optical fibers with anomalous dispersion at 800 nm. *Opt. Lett.* **25**, 25–27 (2000). doi: [10.1364/OL.25.000025](https://doi.org/10.1364/OL.25.000025); pmid: [18059770](https://pubmed.ncbi.nlm.nih.gov/18059770/)
98. L. E. Hargrove, R. L. Fork, M. A. Pollack, Locking of He-Ne laser modes induced by synchronous intracavity modulation. *Appl. Phys. Lett.* **5**, 4–5 (1964). doi: [10.1063/1.1754025](https://doi.org/10.1063/1.1754025)
99. R. L. Fork, B. I. Greene, C. V. Shank, Generation of optical pulses shorter than 0.1 psec by colliding pulse mode locking. *Appl. Phys. Lett.* **38**, 671–672 (1981). doi: [10.1063/1.925000](https://doi.org/10.1063/1.925000)
100. D. E. Spence, P. N. Kean, W. Sibbett, 60-fsec pulse generation from a self-mode-locked Ti:sapphire laser. *Opt. Lett.* **16**, 42–44 (1991). doi: [10.1364/OL.16.000042](https://doi.org/10.1364/OL.16.000042); pmid: [19773831](https://pubmed.ncbi.nlm.nih.gov/19773831/)
101. P. Russell, Photonic crystal fibers. *Science* **299**, 358–362 (2003). doi: [10.1126/science.1079280](https://doi.org/10.1126/science.1079280); pmid: [12532007](https://pubmed.ncbi.nlm.nih.gov/12532007/)
102. U. Morgner *et al.*, Nonlinear optics with phase-controlled pulses in the sub-two-cycle regime. *Phys. Rev. Lett.* **86**, 5462–5465 (2001). doi: [10.1103/PhysRevLett.86.5462](https://doi.org/10.1103/PhysRevLett.86.5462); pmid: [11415276](https://pubmed.ncbi.nlm.nih.gov/11415276/)
103. T. M. Fortier, D. J. Jones, S. T. Cundiff, Phase stabilization of an octave-spanning Ti:sapphire laser. *Opt. Lett.* **28**, 2198–2200 (2003). doi: [10.1364/OL.28.002198](https://doi.org/10.1364/OL.28.002198); pmid: [14649940](https://pubmed.ncbi.nlm.nih.gov/14649940/)
104. T. M. Fortier, A. Bartels, S. A. Diddams, Octave-spanning Ti:sapphire laser with a repetition rate >1 GHz for optical frequency measurements and comparisons. *Opt. Lett.* **31**, 1011–1013 (2006). doi: [10.1364/OL.31.001011](https://doi.org/10.1364/OL.31.001011); pmid: [16599240](https://pubmed.ncbi.nlm.nih.gov/16599240/)
105. R. J. Mears, L. Reekie, I. M. Jauncey, D. N. Payne, Low-noise erbium-doped fibre amplifier operating at 1.54  $\mu\text{m}$ . *Electron. Lett.* **23**, 1026 (1987). doi: [10.1049/el:19870719](https://doi.org/10.1049/el:19870719)
106. J. W. Nicholson *et al.*, All-fiber, octave-spanning supercontinuum. *Opt. Lett.* **28**, 643–645 (2003). doi: [10.1364/OL.28.000643](https://doi.org/10.1364/OL.28.000643); pmid: [12703927](https://pubmed.ncbi.nlm.nih.gov/12703927/)
107. F.-L. Hong *et al.*, Broad-spectrum frequency comb generation and carrier-envelope offset frequency measurement by second-harmonic generation of a mode-locked fiber laser. *Opt. Lett.* **28**, 1516–1518 (2003). doi: [10.1364/OL.28.001516](https://doi.org/10.1364/OL.28.001516); pmid: [12956364](https://pubmed.ncbi.nlm.nih.gov/12956364/)
108. F. Tauser, A. Leitenstorfer, W. Zinth, Amplified femtosecond pulses from an Er:fiber system: Nonlinear pulse shortening and self-referencing detection of the carrier-envelope phase evolution. *Opt. Express* **11**, 594–600 (2003). doi: [10.1364/OE.11.000594](https://doi.org/10.1364/OE.11.000594); pmid: [19461769](https://pubmed.ncbi.nlm.nih.gov/19461769/)
109. B. R. Washburn *et al.*, Phase-locked, erbium-fiber-laser-based frequency comb in the near infrared. *Opt. Lett.* **29**, 250–252 (2004). doi: [10.1364/OL.29.000250](https://doi.org/10.1364/OL.29.000250); pmid: [14759041](https://pubmed.ncbi.nlm.nih.gov/14759041/)
110. T. R. Schibli *et al.*, Frequency metrology with a turnkey all-fiber system. *Opt. Lett.* **29**, 2467–2469 (2004). doi: [10.1364/OL.29.002467](https://doi.org/10.1364/OL.29.002467); pmid: [15584263](https://pubmed.ncbi.nlm.nih.gov/15584263/)

111. S. Droste, G. Ycas, B. Washburn, I. Coddington, N. Newbury, Optical Frequency Comb Generation based on Erbium Fiber Lasers. *Nanophotonics* **5**, 196–213 (2016). doi: [10.1515/nanoph-2016-0019](https://doi.org/10.1515/nanoph-2016-0019)
112. L. C. Sinclair *et al.*, Invited Article: A compact optically coherent fiber frequency comb. *Rev. Sci. Instrum.* **86**, 081301 (2015). doi: [10.1063/1.4928163](https://doi.org/10.1063/1.4928163); pmid: 26329167
113. M. Lezius *et al.*, Space-borne frequency comb metrology. *Optica* **3**, 1381 (2016). doi: [10.1364/OPTICA.3.001381](https://doi.org/10.1364/OPTICA.3.001381)
114. S. A. Diddams, The evolving optical frequency comb. *J. Opt. Soc. Am. B* **27**, B51 (2010). doi: [10.1364/JOSAB.27.000B51](https://doi.org/10.1364/JOSAB.27.000B51)
115. M. E. Fermann, I. Hartl, Ultrafast fibre lasers. *Nat. Photonics* **7**, 868–874 (2013). doi: [10.1038/nphoton.2013.280](https://doi.org/10.1038/nphoton.2013.280)
116. T. Yasui, Y. Kabetani, E. Saneyoshi, S. Yokoyama, T. Araki, Terahertz frequency comb by multifrequency-heterodyning photoconductive detection for high-accuracy, high-resolution terahertz spectroscopy. *Appl. Phys. Lett.* **88**, 241104 (2006). doi: [10.1063/1.2209718](https://doi.org/10.1063/1.2209718)
117. I. A. Finneran *et al.*, Decade-spanning high-precision terahertz frequency comb. *Phys. Rev. Lett.* **114**, 163902 (2015). doi: [10.1103/PhysRevLett.114.163902](https://doi.org/10.1103/PhysRevLett.114.163902); pmid: 25955051
118. F. Adler *et al.*, Phase-stabilized, 1.5 W frequency comb at 2.8–4.8  $\mu\text{m}$ . *Opt. Lett.* **34**, 1330–1332 (2009). doi: [10.1364/OL.34.001330](https://doi.org/10.1364/OL.34.001330); pmid: 19412262
119. A. Schliesser, N. Picqué, T. W. Hänsch, Mid-infrared frequency combs. *Nat. Photonics* **6**, 440–449 (2012). doi: [10.1038/nphoton.2012.142](https://doi.org/10.1038/nphoton.2012.142)
120. A. V. Muraviev, V. O. Smolski, Z. E. Loparo, K. L. Vodopyanov, Massively parallel sensing of trace molecules and their isotopologues with broadband subharmonic mid-infrared frequency combs. *Nat. Photonics* **12**, 209–214 (2018). doi: [10.1038/s41566-018-0135-2](https://doi.org/10.1038/s41566-018-0135-2)
121. G. Ycas *et al.*, High-coherence mid-infrared dual-comb spectroscopy spanning 2.6 to 5.2  $\mu\text{m}$ . *Nat. Photonics* **12**, 202–208 (2018). doi: [10.1038/s41566-018-0114-7](https://doi.org/10.1038/s41566-018-0114-7)
122. A. S. Kowligy *et al.*, Infrared electric field sampled frequency comb spectroscopy. *Sci. Adv.* **5**, eaaw8794 (2019). doi: [10.1126/sciadv.aaw8794](https://doi.org/10.1126/sciadv.aaw8794); pmid: 31187063
123. C. Gohle *et al.*, A frequency comb in the extreme ultraviolet. *Nature* **436**, 234–237 (2005). doi: [10.1038/nature03851](https://doi.org/10.1038/nature03851); pmid: 16015324
124. R. J. Jones, K. D. Moll, M. J. Thorpe, J. Ye, Phase-coherent frequency combs in the vacuum ultraviolet via high-harmonic generation inside a femtosecond enhancement cavity. *Phys. Rev. Lett.* **94**, 193201 (2005). doi: [10.1103/PhysRevLett.94.193201](https://doi.org/10.1103/PhysRevLett.94.193201); pmid: 16090171
125. A. Cingöz *et al.*, Direct frequency comb spectroscopy in the extreme ultraviolet. *Nature* **482**, 68–71 (2012). doi: [10.1038/nature07111](https://doi.org/10.1038/nature07111); pmid: 22297971
126. I. Pupez *et al.*, Compact high-repetition-rate source of coherent 100 eV radiation. *Nat. Photonics* **7**, 608–612 (2013). doi: [10.1038/nphoton.2013.156](https://doi.org/10.1038/nphoton.2013.156)
127. T. Kobayashi, T. Sueta, Y. Cho, Y. Matsuo, High-repetition-rate optical pulse generator using a Fabry-Perot electro-optic modulator. *Appl. Phys. Lett.* **21**, 341–343 (1972). doi: [10.1063/1.1654403](https://doi.org/10.1063/1.1654403)
128. M. Kourogi, B. Widiyatomo, Y. Takeuchi, M. Ohtsu, Limit of optical-frequency comb generation due to material dispersion. *IEEE J. Quantum Electron.* **31**, 2120–2126 (1995). doi: [10.1109/3.477736](https://doi.org/10.1109/3.477736)
129. K. Imai, M. Kourogi, M. Ohtsu, 30-THz span optical frequency comb generation by self-phase modulation in an optical fiber. *IEEE J. Quantum Electron.* **34**, 54–60 (1998). doi: [10.1109/3.655007](https://doi.org/10.1109/3.655007)
130. S. A. Diddams, L.-S. Ma, J. Ye, J. L. Hall, Broadband optical frequency comb generation with a phase-modulated parametric oscillator. *Opt. Lett.* **24**, 1747–1749 (1999). doi: [10.1364/OL.24.001747](https://doi.org/10.1364/OL.24.001747); pmid: 18079922
131. M. Zhang *et al.*, Broadband electro-optic frequency comb generation in a lithium niobate microring resonator. *Nature* **568**, 373–377 (2019). doi: [10.1038/s41586-019-1008-7](https://doi.org/10.1038/s41586-019-1008-7); pmid: 30858615
132. I. Morohashi *et al.*, Widely repetition-tunable 200 fs pulse source using a Mach-Zehnder-modulator-based flat comb generator and dispersion-flattened dispersion-decreasing fiber. *Opt. Lett.* **33**, 1192–1194 (2008). doi: [10.1364/OL.33.001192](https://doi.org/10.1364/OL.33.001192); pmid: 18516170
133. A. Ishizawa *et al.*, Generation of 120-fs laser pulses at 1-GHz repetition rate derived from continuous wave laser diode. *Opt. Express* **19**, 22402–22409 (2011). doi: [10.1364/OE.19.022402](https://doi.org/10.1364/OE.19.022402); pmid: 22109116
134. A. J. Metcalf, V. Torres-Company, D. E. Leaird, A. M. Weiner, High-power broadly tunable electrooptic frequency comb generator. *IEEE J. Sel. Top. Quantum Electron.* **19**, 231–236 (2013). doi: [10.1109/JSTQE.2013.2268384](https://doi.org/10.1109/JSTQE.2013.2268384)
135. K. Beha *et al.*, Electronic synthesis of light. *Optica* **4**, 406 (2017). doi: [10.1364/OPTICA.4.000406](https://doi.org/10.1364/OPTICA.4.000406)
136. D. R. Carlson *et al.*, Ultrafast electro-optic light with subcycle control. *Science* **361**, 1358–1363 (2018). doi: [10.1126/science.aat6451](https://doi.org/10.1126/science.aat6451); pmid: 30262499
137. T. J. Kippenberg, R. Holzwarth, S. A. Diddams, Microresonator-based optical frequency combs. *Science* **332**, 555–559 (2011). doi: [10.1126/science.1193968](https://doi.org/10.1126/science.1193968); pmid: 21527707
138. D. K. Armani, T. J. Kippenberg, S. M. Spillane, K. J. Vahala, Ultra-high-Q toroid microcavity on a chip. *Nature* **421**, 925–928 (2003). doi: [10.1038/nature01371](https://doi.org/10.1038/nature01371); pmid: 12606995
139. K. J. Vahala, Optical microcavities. *Nature* **424**, 839–846 (2003). doi: [10.1038/nature01939](https://doi.org/10.1038/nature01939); pmid: 12917698
140. I. S. Grudinin, V. S. Ilchenko, L. Maleki, Ultrahigh optical Q factors of crystalline resonators in the linear regime. *Phys. Rev. A* **74**, 063806 (2006). doi: [10.1103/PhysRevA.74.063806](https://doi.org/10.1103/PhysRevA.74.063806)
141. J. S. Levy *et al.*, CMOS-compatible multiple-wavelength oscillator for on-chip optical interconnects. *Nat. Photonics* **4**, 37–40 (2010). doi: [10.1038/nphoton.2009.259](https://doi.org/10.1038/nphoton.2009.259)
142. Q. Li *et al.*, Stably accessing octave-spanning microresonator frequency combs in the soliton regime. *Optica* **4**, 193–203 (2017). doi: [10.1364/OPTICA.4.000193](https://doi.org/10.1364/OPTICA.4.000193); pmid: 28603754
143. T. J. Kippenberg, S. M. Spillane, K. J. Vahala, Kerr-nonlinear optical parametric oscillation in an ultrahigh-Q toroid microcavity. *Phys. Rev. Lett.* **93**, 083904 (2004). doi: [10.1103/PhysRevLett.93.083904](https://doi.org/10.1103/PhysRevLett.93.083904); pmid: 15447188
144. A. A. Savchenko *et al.*, Low threshold optical oscillations in a whispering gallery mode  $\text{CaF}_2$  resonator. *Phys. Rev. Lett.* **93**, 243905 (2004). doi: [10.1103/PhysRevLett.93.243905](https://doi.org/10.1103/PhysRevLett.93.243905); pmid: 15697815
145. P. Del'Haye *et al.*, Optical frequency comb generation from a monolithic microresonator. *Nature* **450**, 1214 (2007).
146. S. Wabnitz, Suppression of interactions in a phase-locked soliton optical memory. *Opt. Lett.* **18**, 601 (1993). doi: [10.1364/OL.18.000601](https://doi.org/10.1364/OL.18.000601); pmid: 19802213
147. F. Leo *et al.*, Temporal cavity solitons in one-dimensional Kerr media as bits in an all-optical buffer. *Nat. Photonics* **4**, 471–476 (2010). doi: [10.1038/nphoton.2010.120](https://doi.org/10.1038/nphoton.2010.120)
148. T. Herr *et al.*, Temporal solitons in optical microresonators. *Nat. Photonics* **8**, 145–152 (2014). doi: [10.1038/nphoton.2013.343](https://doi.org/10.1038/nphoton.2013.343)
149. X. Yi, Q.-F. Yang, K. Y. Yang, M.-G. Suh, K. Vahala, Soliton frequency comb at microwave rates in a high-Q silica microresonator. *Optica* **2**, 1078 (2015). doi: [10.1364/OPTICA.2.001078](https://doi.org/10.1364/OPTICA.2.001078)
150. C. Joshi *et al.*, Thermally controlled comb generation and soliton modelocking in microresonators. *Opt. Lett.* **41**, 2565–2568 (2016). doi: [10.1364/OL.41.002565](https://doi.org/10.1364/OL.41.002565); pmid: 27244415
151. P.-H. Wang *et al.*, Intracavity characterization of micro-comb generation in the single-soliton regime. *Opt. Express* **24**, 10890–10897 (2016). doi: [10.1364/OE.24.010890](https://doi.org/10.1364/OE.24.010890); pmid: 27409909
152. T. J. Kippenberg, A. L. Gaeta, M. Lipson, M. L. Gorodetsky, Dissipative Kerr solitons in optical microresonators. *Science* **361**, eaan8083 (2018). doi: [10.1126/science.aan8083](https://doi.org/10.1126/science.aan8083); pmid: 30093576
153. Y. Okawachi *et al.*, Octave-spanning frequency comb generation in a silicon nitride chip. *Opt. Lett.* **36**, 3398–3400 (2011). doi: [10.1364/OL.36.003398](https://doi.org/10.1364/OL.36.003398); pmid: 21886223
154. V. Brasch *et al.*, Photonic chip-based optical frequency comb using soliton Cherenkov radiation. *Science* **351**, 357–360 (2016). doi: [10.1126/science.aad4811](https://doi.org/10.1126/science.aad4811); pmid: 26721682
155. M. H. P. Pfeiffer *et al.*, Octave-spanning dissipative Kerr soliton frequency combs in  $\text{Si}_3\text{N}_4$  microresonators. *Optica* **4**, 684 (2017). doi: [10.1364/OPTICA.4.000684](https://doi.org/10.1364/OPTICA.4.000684)
156. Z. Gong *et al.*, High-fidelity cavity soliton generation in crystalline AlN micro-ring resonators. *Opt. Lett.* **43**, 4366–4369 (2018). doi: [10.1364/OL.43.004366](https://doi.org/10.1364/OL.43.004366); pmid: 30211865
157. Y. He *et al.*, Self-starting bi-chromatic LiNbO<sub>3</sub> soliton microcomb. *Optica* **6**, 1138 (2019). doi: [10.1364/OPTICA.6.001138](https://doi.org/10.1364/OPTICA.6.001138)
158. L. Chang *et al.*, Ultra-efficient frequency comb generation in AlGaAs-on-insulator microresonators. *Nat. Commun.* **11**, 1331 (2020). doi: [10.1038/s41467-020-15005-5](https://doi.org/10.1038/s41467-020-15005-5); pmid: 32165610
159. D. T. Spencer *et al.*, An optical-frequency synthesizer using integrated photonics. *Nature* **557**, 81–85 (2018). doi: [10.1038/s41586-018-0065-7](https://doi.org/10.1038/s41586-018-0065-7); pmid: 29695870
160. S. B. Papp *et al.*, Microresonator frequency comb optical clock. *Optica* **1**, 10 (2014). doi: [10.1364/OPTICA.1.000010](https://doi.org/10.1364/OPTICA.1.000010)
161. Z. L. Newman *et al.*, Architecture for the photonic integration of an optical atomic clock. *Optica* **6**, 680 (2019). doi: [10.1364/OPTICA.6.000680](https://doi.org/10.1364/OPTICA.6.000680)
162. M.-G. Suh *et al.*, Searching for exoplanets using a microresonator astrocomb. *Nat. Photonics* **13**, 25–30 (2019). doi: [10.1038/s41566-018-0312-3](https://doi.org/10.1038/s41566-018-0312-3); pmid: 30740138
163. E. Obrzud *et al.*, A microphotonic astrocomb. *Nat. Photonics* **13**, 31–35 (2019). doi: [10.1038/s41566-018-0309-y](https://doi.org/10.1038/s41566-018-0309-y)
164. P. Marin-Palomero *et al.*, Microresonator-based solitons for massively parallel coherent optical communications. *Nature* **546**, 274–279 (2017). doi: [10.1038/nature22387](https://doi.org/10.1038/nature22387); pmid: 28593968
165. M.-G. Suh, Q.-F. Yang, K. Y. Yang, X. Yi, K. J. Vahala, Microresonator soliton dual-comb spectroscopy. *Science* **354**, 600–603 (2016). doi: [10.1126/science.aah6516](https://doi.org/10.1126/science.aah6516); pmid: 27738017
166. M. Yu *et al.*, Silicon-chip-based mid-infrared dual-comb spectroscopy. *Nat. Commun.* **9**, 1869 (2018). doi: [10.1038/s41467-018-04350-1](https://doi.org/10.1038/s41467-018-04350-1); pmid: 29760418
167. M.-G. Suh, K. J. Vahala, Soliton microcomb range measurement. *Science* **359**, 884–887 (2018). doi: [10.1126/science.aao1968](https://doi.org/10.1126/science.aao1968); pmid: 29472476
168. P. Trocha *et al.*, Ultrafast optical ranging using microresonator soliton frequency combs. *Science* **359**, 887–891 (2018). doi: [10.1126/science.aao3924](https://doi.org/10.1126/science.aao3924); pmid: 29472477
169. J. N. Eckstein, A. I. Ferguson, T. W. Hänsch, High-resolution two-photon spectroscopy with picosecond light pulses. *Phys. Rev. Lett.* **40**, 847–850 (1978). doi: [10.1103/PhysRevLett.40.847](https://doi.org/10.1103/PhysRevLett.40.847)
170. M. J. R. Heck *et al.*, Hybrid silicon photonic integrated circuit technology. *IEEE J. Sel. Top. Quantum Electron.* **19**, 6100117 (2013). doi: [10.1109/JSTQE.2012.2235413](https://doi.org/10.1109/JSTQE.2012.2235413)
171. P. Manurkar *et al.*, Fully self-referenced frequency comb consuming 5 Watts of electrical power. *OSA Continuum* **1**, 274 (2018). doi: [10.1364/OSAC.1.000274](https://doi.org/10.1364/OSAC.1.000274)
172. T. C. Briles *et al.*, Interlocking Kerr-microresonator frequency combs for microwave to optical synthesis. *Opt. Lett.* **43**, 2933–2936 (2018). doi: [10.1364/OL.43.002933](https://doi.org/10.1364/OL.43.002933); pmid: 29905727
173. D. R. Carlson *et al.*, Photonic-chip supercontinuum with tailored spectra for counting optical frequencies. *Phys. Rev. Appl.* **8**, 014027 (2017). doi: [10.1103/PhysRevApplied.8.014027](https://doi.org/10.1103/PhysRevApplied.8.014027)

## ACKNOWLEDGMENTS

We are grateful to T. Hänsch and J. Hall for their input, vision, and leadership in this field, as well as to N. Newbury, C. Oates, and J. Ye for their comments on this manuscript. We also thank B. Baxley, T. Briles, J. Knight, S. Papp, P. Russell, R. Windeler, and the University of Bath for their contributions to the figures. Finally, we are indebted to the many colleagues with whom we have had the privilege to learn about the ever-expanding field of optical frequency combs. **Funding:** This material is based on work supported by the National Institute of Standards and Technology (NIST); the Defense Advanced Research Projects Agency (DARPA) under awards in the DODOS (HRO01-15-C-0055), APHI (FA9453-19-C-0029), SCOUT (W31P4Q-15-1-0011), and ACES programs; and the Air Force Office of Scientific Research (AFOSR) under awards FA9550-16-1-0016 and FA9550-18-1-0353. **Competing interests:** T.U. is an inventor on patents US6785303B1 and US20060268949 held by the Max-Planck-Gesellschaft zur Förderung der Wissenschaften that cover optical frequency combs.

10.1126/science.aay3676

## Optical frequency combs: Coherently uniting the electromagnetic spectrum

Scott A. Diddams, Kerry Vahala and Thomas Udem

*Science* **369** (6501), eaay3676.  
DOI: 10.1126/science.aay3676

### An optical timekeeper

Optical clocks, based on optical transitions of atoms, operate at much higher frequency than the microwave atomic clocks currently used as our timing standards. They have been shown to exhibit better stability and are poised to redefine the second. The development of stable, self-referenced optical frequency combs that span the microwave to optical wavelengths has been key to these efforts. Diddams *et al.* reviewed developments and refinements of these optical combs over the past 20 years and provide an overview of where they are finding application, from precision timing to high-resolution spectroscopy and imaging, ranging, and navigation.

*Science* this issue p. eaay3676

#### ARTICLE TOOLS

<http://science.sciencemag.org/content/369/6501/eaay3676>

#### REFERENCES

This article cites 164 articles, 16 of which you can access for free  
<http://science.sciencemag.org/content/369/6501/eaay3676#BIBL>

#### PERMISSIONS

<http://www.sciencemag.org/help/reprints-and-permissions>

Use of this article is subject to the [Terms of Service](#)

---

*Science* (print ISSN 0036-8075; online ISSN 1095-9203) is published by the American Association for the Advancement of Science, 1200 New York Avenue NW, Washington, DC 20005. The title *Science* is a registered trademark of AAAS.

Copyright © 2020 The Authors, some rights reserved; exclusive licensee American Association for the Advancement of Science. No claim to original U.S. Government Works